THE ROLE OF PROLACTIN RECEPTOR SIGNALING IN LIVER HOMEOSTASIS AND DISEASE

by

Jennifer Abla Yanum

A Thesis

Submitted to the Faculty of Purdue University

In Partial Fulfillment of the Requirements for the degree of

Master of Science

Department of Biology at IUPUI

Indianapolis, Indiana

August 2021

THE PURDUE UNIVERSITY GRADUATE SCHOOL
STATEMENT OF COMMITTEE APPROVAL

Dr. Guoli Dai, Chair
Department of Biology

Dr. James Marrs
Department of Biology

Dr. Lata Balakrishnan
Department of Biology

Approved by:
Dr. Theodore Cummins

To God and family

ACKNOWLEDGMENTS

I genuinely want to express my gratitude to Dr. Guoli Dai for accepting me to be a part of his laboratory and for his constant guidance and mentorship. I would like to thank him for believing in me and helping me accomplish my life goals. I would also like to thank Dr. James Marrs and Dr. Lata Balakrishnan for accepting to serve on my committee, for their insightful suggestions and inputs on how to make my research better. Worth mentioning are my fellow lab members Dr. Joonyong Lee, Dr. Huaizhou Jiang, Dr. Shashank Nambiar and Veronica Garcia for helping with data collection, analysis and teaching me most of the skills I have acquired. Without your help I could not have come this far. Thank you! Again, to Dr. Michael Soares of the Department of Pathology and Laboratory Medicine at the University of Kansas Medical Center, Kansas City, USA for gifting us *Prlr*-floxed mice. I would also like to acknowledge Dr. Kathleen Marrs and Mrs. Laura Flak for being super kind and for their continuous support and encouragement. Finally, to my parents and family especially Victor Afun, Felix Yanum and Mark-Eric Adzadza; for their love and prayers, and to everyone who helped me along this journey, I am truly grateful.

TABLE OF CONTENTS

LIST OF TABLES

LIST OF FIGURES

ABSTRACT

Functioning as a "powerhouse", the liver adapts to the metabolic needs of the body by maintaining a homeostatic balance. Prolactin receptor (PRLR) has been found to have a copious existence in the liver. Having established a well-defined role in both reproductive and endocrine systems, the role of this transmembrane protein in hepatocytes is yet to be elucidated. Due to its abundant nature, we hypothesized that PRLR is required for maintaining hepatic homeostasis and plays a role in liver diseases. To test this hypothesis, we defined two specific aims. The first was to explore whether PRLR loss-of-function affects liver structure and function in physiological conditions. The second was to determine whether PRLR is associated with liver pathology. We deleted the *Prlr* gene specifically in hepatocytes using a virus-based approach and evaluated liver function, transcriptome, and activities of downstream signaling molecules. Due to the absence of PRLR, we found that the urea cycle was disrupted, concomitant with excessive accumulation of urea in the blood; 133 genes exhibited differential expression, largely associated with hepatocyte structure, metabolism, and inflammation; and the activities of STAT3 and 5 were reduced. The results signify that PRLR indeed plays a homeostatic role in the liver. We also used $Prlr^{+/-}$ mice to assess whether the loss of one allele of the *Prlr* gene alters maternal hepatic adaptations to pregnancy. As a result, in the pre-pregnancy state and during the first half of gestation, the expression of maternal hepatic PRLR protein was reduced approximately by half owing to *Prlr* insufficiency. However, during the second half of pregnancy, we observed compensatory upregulation of this molecule, leading to minimal interference in STAT 3 and 5 signaling and liver size. Contrary to a previous study in the breast and ovary, our results suggest that one allele of *Prlr* may be sufficient for the maternal liver to respond to this physiological stimulus (pregnancy). Furthermore, we examined the expression and activity of PRLR in fatty as well as cholestatic livers. Using a high fat diet, we induced non-alcoholic fatty liver disease (NAFLD). Strikingly and for the first time, we discovered that the short isoform of PRLR (PRLR-S) was completely inactivated in response to NAFLD, whereas the long isoform remained unchanged. This finding strongly suggests the involvement of PRLR-S in lipid metabolism. We also postulate that PRLR-L may be the major regulator of STAT signaling in the liver, consistent with other reports. Lastly, we induced extrahepatic cholestasis via bile duct ligation (BDL) in mice. As this liver disease progressed, the expression of both isoforms

of PRLR generally declined and was surprisingly accompanied by increased STAT 3 and 5 activity. The data suggests that PRLR participates in this disease progression, with a disconnection between PRLR signaling and STAT proteins. Collectively, our preliminary studies suggest that PRLR signaling is required to maintain liver homeostasis and more prominently, is involved in liver diseases, especially NAFLD. These findings lay a foundation for our future studies.

CHAPTER 1. INTRODUCTION

1.1 Background

For the many physiological processes required to maintain homeostasis in the body, the multifaceted and dynamic structure of the liver comes to play with a highly significant role. The liver has structurally and functionally heterogeneous characteristics which enable it to adapt to the various demands of the body. Liver diseases such as alcoholic liver disease (ALD), non -alcoholic fatty liver disease (NAFLD), hepatitis and liver cirrhosis are largely on the rise and mostly instigated by lifestyle; which remains a global health concern[1]. Liver diseases usually begin with an inflammation to the liver, progressing to scarring known as fibrosis, cirrhosis, end-stage liver failure and eventually liver cancer. In recent times, studies have projected NAFLD to soon overtake hepatitis C, thereby becoming the prevalent form of chronic hepatic disease; with a clinico-pathological spectrum developed about its line of action[2]. Risk factors such as dyslipidemia, diabetes and obesity can cause injury to a healthy liver which induces steatosis with no hepatocellular damage (NAFLD). This is more susceptible in men than in women. NAFLD in turn progresses into an aggressive variant; non-alcoholic steatohepatitis (NASH), that is steatosis concurrent with liver injury and lobular inflammation. These two conditions are reversible with early detection; otherwise, liver cirrhosis occurs progressing to hepatocellular carcinoma with a sole remedy of transplant to resolve this[3, 4]. There is however an urgent need to develop some new experimental therapies to fight this.

1.2 Anatomy of the liver

The gross anatomy of this organ reveals a dark reddish-brown conical structure which derives its pigmentation from being highly vascularized and is known as the largest mammalian gland in the body[5]. Weighing approximately 1500g in humans and 2-3g in mice, it is situated in the upper-right quadrant of the abdominal cavity, beneath the diaphragm and slightly above the right kidney and intestines, which corroborates its existence as an accessory organ of digestion. It extends across the hypochondria and epigastric region; mainly occupying the right hypochondrium. The number of lobes the liver has depends on one's anatomical view. Its superior surface is attached to the diaphragm via the falciform ligament which divides it into two lobes: the left and the right

lobes with the latter being larger in size. Viscerally, the liver is divided into two accessory lobes; the caudate and quadrate lobes located beneath the right lobe. The round ligament of the liver; ligamentum teres hepatis, divides the left lateral lobe into the medial and lateral segments and connects the liver to the umbilicus. Another ligament known as the ligamentum venosum is continuous with the round ligament and forms part of the left branch of the portal vein. Cantlie's line, a plane which runs through the gall bladder and caudate lobe, towards the vena cava functionally divides the liver into two lobes with the hepatic vein lying within this plane[6]. The gallbladder; responsible for storing bile duct produced by the liver lies beneath the liver and is connected via the common hepatic duct. In all, the liver is divided into five main lobes and eight segments according to the Couinaud system[7], shown in **Figure 1**.

1.3 Structural unit of the liver

The basic functional unit of the liver known as the lobule, is a hexagonal structure. The vertices of this hexagonal unit comprise a network made up of two inlets (hepatic artery and portal vein) and an outlet (bile duct). Together, these outlets form the portal triad whose main function is to form the vasculature of the liver. The hepatic artery supplies oxygenated blood to the liver whilst the portal vein supplies deoxygenated blood to the liver. The two forms of blood mix at a junction known as the sinusoid which forms the microvasculature and is widely distributed across the liver. The core of the lobule is made up of a structure which carries blood from the liver to the inferior vena cava of the heart and is known as the central vein[8]. Thousands of hepatocytes make up the lobules which in turn make up the volume of the liver. Being oriented around the afferent vascular system, the hepatic acinus of the liver becomes the functional blood flow unit of the liver[9].

1.3.1 Liver zonation

Due to the functional and structural unit of the acinus of the liver, a highly specialized phenomenon termed metabolic zonation has been identified; depending on the distance from arterial blood supply[10]. Optimization of hepatic functions however depends on the zonal distribution of metabolic tasks which are non-uniformly distributed. Zonation has since been attributed to the oxygen gradient created during blood flow across the radial axis of liver lobules but recent research [11] has demonstrated that genes responsible for zonation such as those in Wnt signaling (a major

regulator of zonation[12]) and Hedgehog signaling may be regulated by a hypoxia signaling pathway and its inducible transcription factors. Again, single-cell transcriptomics have revealed that approximately 50% of genes expressed in the mouse liver are zonated with spatial and heterogeneous profiling whereas the heterogeneity is an effect of gradients of oxygen, nutrients, hormones and interaction between epigenetic markers of hepatic cells[13]. Metabolic zonation has been demonstrated by many pathways such as carbohydrates, lipids and xenobiotics metabolic pathways[14, 15], however it is shown to be dynamic since gene expression changes occur due to response to drugs, diet, environment and hormones[16]. This phenomenon is however not fully elucidated as at now due to discrepancies in mouse and human models[13].

Zone 1 of the liver encircles the portal triad in the periportal zone; at the site where oxygenated blood enters via the hepatic artery. Due to its oxygenation, it is the most resistant to ischemia but is usually the first site to be affected by drug hepatotoxicity and viral hepatitis. It is particularly involved in gluconeogenesis, urea, and cholesterol biosynthesis[15, 17].

Zone 2, midlobular with sub-optimal levels of oxygen forms the intermediate zone. It is a transitional zone with functions consistent with both zones 1 and 2 and is the site affected by yellow fever[11, 18].

Zone 3, the perivenous (pericentral or centrilobular) region forms around the central veins where oxygenation is poor, which makes it the most susceptible to ischemic attacks. However, it has abundant levels of Cytochrome P450, an oxidative group of enzymes responsible for xenobiotic metabolism of compounds thereby enhancing drug half-life. Zone 3 is also active in glycolysis; an opposing pathway to that found in the periportal region (zone 1), as well as glutamine [19] and bile acid biosynthesis.

The opposing functions in these zones further complements the spatial heterogeneity of the liver which helps to prevent competition for the same substrate; thereby regulating liver homeostasis.

1.4 Microanatomy of the liver

The cells of the liver are distinguished by a parenchymal or non-parenchymal classification. Parenchymal cells constitute 80% of the mass of a liver making up 60% of its composition. These cells are known as hepatocytes and perform most functions of the liver. Hepatic stellate cells,

Kupffer cells, cholangiocytes or biliary epithelial cells, sinusoidal endothelial cells and intrahepatic lymphocytes make up 40% of hepatic cellular composition and belong to the non-parenchymal cell (NPC) population[20]. The presence of NPC's improves the physiological relevance of parenchymal cells by secreting factors that influence transportation, growth, and metabolic functions of hepatocytes; primary hepatocyte toxicity testing has confirmed[21].

1.4.1 Parenchymal cells

Primarily consisting of polygonal epithelial cells (hepatocytes), they make up the primary epithelial cell population of the liver which are arranged in thousands of polyhedral lobules with cords which radiate towards the central vein. They contain large nuclei (as shown by arrows in **Figure 2**) which are centrally placed, can occur in pairs (binucleation), and involved in a series of interconnected endocrine, metabolic and secretory functions.

Production: hepatocytes produce bile, passes it through tiny vessels which run parallel to sinusoids known as bile canaliculi and these are collected into the bile ducts for transport into the gall bladder for storage and digestion. They also synthesize plasma proteins involved in blood coagulation such as albumins, fibrinogen, prothrombin, and globulins.

Metabolism: hepatocytes are fed with blood from the hepatic portal vein which causes their intricate involvement in carbohydrate, protein, and lipid metabolism. They also breakdown hemoglobin into heme and globulin components; with globulin further broken down to produce sources of energy and heme converted into bilirubin which gives bile its green pigmentation.

Detoxification: with the help of liver enzymes, hepatocytes filter the blood to get rid of potential toxins to the body such as alcohol and drugs by inactivating them[22]. They also deaminate amino acids and convert them into urea to be excreted.

Storage: they store folic acid, vitamins such as Vitamin B12 and minerals such as copper and iron. Also, they store glucose in the form of glycogen, proteins as amino acids and lipids as fatty acids which are required for ATP release and daily functioning of the body.

1.4.2 Non-parenchymal cells

Cholangiocytes: cholangiopathies account for a substantial percentage of liver transplants which iterates the relevance of cholangiocytes[23]. Lining the lumen of bile ducts, these cuboidal structures make up the second most abundant epithelial cell population in the liver, contributing to bile secretion and active transport of electrolytes. Biliary epithelial cells (BECs), shown in **Figure 2** actively modify bile during its transport via secretion of bicarbonates which regulate the PH of bile as well as absorption of bile acids, amino acids, ions and other molecules[24].

Hepatic stellate cells: also known as Ito cells or lipocytes, they can switch between a quiescent and activated state depending on the state of the liver; healthy or injured. Histologically, they appear as large lipid vacuoles which store fats. Lying in the peri-sinusoidal region called Space of Disse; a region between endothelial cells and hepatocytes, they regulate sinusoidal blood flow and produce extracellular matrix (Collagen types I and III). They store retinol (Vitamin A) in lipid droplets in their quiescent state and upon activation, set in motion by liver injury, they respond to pro-fibrogenic factors such as transforming growth factor-β (TGF-β) which induces tissue repair thereby causing them to lose the Vitamin A stores. The extracellular matrix they produce is in response to liver injury where they proliferate to deposit and organize collagen in the injured tissue eventually leading to scarring[25].

Kupffer cells: they descend from the monocytic lineage and differentiate into macrophages which line the endothelial surfaces of sinusoids, sharing proximity with the portal triad. They function in engulfing senescent red blood cells as well as pathogenic materials from the gut which enter the liver through the portal blood vessels. They are only visible histologically as round cells when they contain phagocytosed material. They also serve as Antigen Presenting Cells (APCs) in adaptive immunity thereby secreting proinflammatory cytokines and chemokines in the liver.

Oval cells: these are the pluripotent stem cells of the liver which are involved in differentiating to populate hepatocytes and capable of transdifferentiating into other lineages such as biliary epithelial cells, post injury to the liver. They are mainly seen post-injury to the liver in adults. Immunohistochemistry studies in rats showed that oval cells express a lineage specific marker, Thy-1 antigen which is normally expressed in fetal liver and hardly found in adult liver[26]. Work done by Fausto et al revealed that, oval cells differentiate into hepatocytic lineages only when

hepatocyte proliferation is delayed or blocked whilst compensatory hyperplasia (proliferation by hepatocytes) is the major phenomenon observed in liver regeneration post liver damage[27].

Sinusoidal endothelial cells: responsible for transporting blood throughout the liver, they are specialized endothelial cells which form fenestrated sieve plates (a single layer with spaces between each cell) in the sinusoidal lumen necessary for exchange of proteins and essential materials between hepatocytes and blood plasma. Aside filtration of blood, they perform sentinel functions in conjunction with Kupffer cells by recruiting leukocytes, presentation of antigen and an overall maintenance of immune homeostasis in the liver[28].

Intrahepatic lymphocytes: these are also known as pit cells which inhabit the sinusoids occasionally to contribute to immunity. Supported by the presence of Recombinase-activating genes (RAGs 1 and 2), a look into the origin of these cells showed that some T cells can mature in a thymus-independent fashion in the liver and attain a non-circulating existence[29, 30].

1.4.3 Other components

Innervation: the liver receives a supply of both afferent and efferent nerve supply which helps in regulating liver homeostasis. Although evidence of hepatic innervation is species dependent[31], parasympathetic denervation of the liver has been seen to disrupt glucose[32] and lipid metabolism[33], with vagotomy also impairing DNA synthesis and mass restoration in liver regeneration studies post partial hepatectomy[34], in both murine and human subjects[35].

1.5 Liver regeneration

As a vital organ required for maintaining homeostasis and regulating body functions, dysfunction in any of its processes is detrimental and can lead to hepatic encephalopathy, a condition which causes toxin build-up concurrent with a decline in brain function; consequently, leading to a coma. Fortunately, the unique and dynamic ability of this organ to regenerate helps to restore that homeostatic balance. Chemical[36] and physical injury[37] to the liver have been observed to effect a regenerative response, however, a model first described by Higgins in 1931 in rats [38] has been accepted as the standard method of studying liver regeneration; two-thirds partial hepatectomy (2/3 PHx). Although widely accepted, this procedure has however been revised and

improvised to attain reproducible and consistent results across all species and labs studying this phenomenon, mainly because of the structural anatomy of organs in different species (rats do not possess a gall bladder like mice do[39]).

1.5.1 The partial hepatectomy model

2/3 PHx involves a laparotomy-based resection of approximately 70% of the liver; both median lobes and the left lateral lobe. Many factors influence a good regenerative outcome, the surgical procedure, choice of anesthesia, diet or fasting state, sex, and the age of mice. Work done by Polina Iakova demonstrated a C/EBPα repression pathway switching effect in older mice which causes repression of E2F transcriptional genes (required for proliferation), instead of repressing cyclin dependent kinases and in effect diminishes the regenerative capability in older mice[40]. The 2/3 PHx model thereby admonishes the use of mice between 8 to 14 weeks for regeneration studies[39]. Again, variability in the proliferative ability of hepatocytes in male and female mice post hepatectomy was observed by a group in 2006 who used liver-specific "insulin-like growth factor 1" (IGF-1) knockout mice and this caused a diminished regenerative effect in males[41]. It is therefore imperative to study sex-dependent effects caused by genetic modifications in regeneration studies. Disruption of adipogenesis occurs in mice which are fasted prior to partial hepatectomy procedures; induction of hepatic steatosis occurs which limits the regenerative capability of the liver[42]. The standardized model advises maintenance of the metabolic state in mice before surgical procedures are carried out[39]. Considering the xenobiotic detoxification function of the liver, it is crucial to use anesthesia which causes minimal to no hepatotoxicity in mice. Isoflurane has been determined to be a suitable choice of anesthesia for partial hepatectomy surgeries, with ideal properties and an easy mode of administration via inhalation[43, 44].

1.5.2 Factors associated with liver regeneration

A combination of cytokines, hemodynamic changes, hepatic growth factors, signaling pathways, genes and transcription factors have been found to contribute to the regenerative capability of hepatocytes although not completely elucidated. Partial hepatectomy-induced regeneration initiates DNA synthesis in numerous cell types across the organ; both parenchymal and non-parenchymal, with hepatocytes priming this compensatory hyperplasia. Quiescent hepatocytes

(hepatic progenitor cells) get activated and enter the cell cycle post hepatectomy to repopulate hepatocytes alongside matrix remodeling to restore liver mass. Many publications on liver regeneration record the non-involvement of hepatic oval cells however, recent research explains three different mechanisms of liver regeneration depending on the severity of liver injury and damage to hepatocytes: compensatory hyperplasia by hepatocytes, extrahepatic stem cell induced regeneration (trans-differentiation) and hepatocytic stem cell mediated regeneration[45]. Nonetheless, the actual mechanism of action by stem cells are not well understood as to whether they support parenchymal cells via cytokine release or actual differentiation into hepatocytes. Hepatocyte entry into the cell cycle to begin proliferation post hepatectomy occurs with a peak in DNA synthesis by 36 hours, with restoration of full liver mass approximately a week after the procedure. This can be assessed by BrdU or Ki67 incorporation into regenerated hepatocytes. A couple of molecular pathways such as the Ras/Raf pathway, the JAK/STAT pathway, the PI3K/AKT pathway, NF-kb, Hippo signaling pathway and Wnt/β-catenin pathway crosstalk to enhance proliferation, de-differentiation and cell survival post-surgery[37].

The hemostatic system has also been linked to play a significant role in liver regeneration[46]. Due to the massive supply of blood to the liver through the portal vein, resection of 70% of the lobes induces a shear stress on sinusoids by increasing the volume of blood flow per sinusoid thereby increasing sinusoidal diameter, widening the Space of Disse and distorting the fenestrated appearance until about the ten-day liver mass recovery[47]. The increased shear stress compliments hepatocyte proliferation to restore liver mass. Regrowth of other cell population like the cholangiocytes and sinusoidal endothelial cells occur from mature cholangiocytes and bone marrow sinusoidal precursors respectively in the remnant liver after hepatocyte proliferation takes place, with a peak in three days[48-50].

It is however intriguing to know that some physiological states can improve the molecular mechanisms governing proliferation of hepatocytes post-hepatectomy. We recently studied the effects of pregnancy on partial-hepatectomy induced regeneration and demonstrated that pregnancy induces hepatic steatosis and initiates an early entry into the S phase of the cell cycle post resection, with an overall enhanced state of mitogenesis[51]. Western blot analysis also revealed EGFR, STAT 5 and c-met as critical players in liver regeneration.

1.6 Prolactin receptor (PRLR)

PRLR exhibits pleiotropism; a unique feature which allows for the activation of several signaling pathways. It is widely expressed across many tissues in the body as membrane-bound or in a soluble form (PRL-binding protein), owing to being transcriptionally regulated by three different promoters. Promoter I is found to be gonad specific, II is liver specific and III represents both gonadal and non-gonadal tissue regulation. It is highly abundant in the ovary, mammary gland, the central nervous system, liver, pancreas, spleen, and skeletal muscle. Belonging to the type 1 group of hematopoietic cytokine receptors and being a single-pass transmembrane receptor, it can bind to and become activated by a triad of hormones or ligands which stem from a common ancestral descent and later diverged; the prolactin hormone (PRL), growth hormone (GH) and placental lactogen (PL). Out of these three ligands, prolactin tends to bind to PRLR at a higher affinity than the other two ligands. Placental lactogen is mainly secreted in response to gestation whilst the expression levels of growth hormone are relatively lower than prolactin and is species dependent. In humans, the gene encoding PRLR is located on chromosome 5 and found on chromosome 15 in mice[52]. It spans across a length exceeding 100kb and contains at least 10 exons. Multiple isoforms of PRLR exist depending on the species, with a difference in the length of their cytoplasmic tails and this is as a result of alternative initiation sites, post-translational modifications (such as glycosylation, proteolytic cleavage, and phosphorylation) as well as differential RNA splicing events; which causes them to vary in the length of their intracellular domains as well. In humans and rats, three isoforms (short, intermediate, and long forms) have been identified. In mice, two isoforms (one long and three short forms) have been recorded also due to differences in their intracellular domain[53] however, they maintain a uniform extracellular domain across all isoforms. Expression of these isoforms vary depending on the estrous cycle, lactation, pregnancy**[54, 55]** and metabolism (newly discovered unpublished lab data;4.3).

1.6.1 PRL-the paramount activator of PRLR

PRL is a hormone secreted by the lactotroph cells of the adenohypophysis and classified as a class 1 cytokine protein. PRL is found on chromosome 6 (having 5 exons and 4 introns) in humans and chromosome 13 in mice with a molecular mass of approximately 23kDa and 22kDa, respectively. Transcription of prolactin is regulated by two promoters; the proximal promoter and the

extrapituitary promoter region. It is inhibited by dopamine, a secretion from the hypothalamus of the brain. Being famous for its role in lactation, its discovery across many tissues have helped the recognition of over three hundred roles associated with this hormone [56] (with some categorizations below), and accomplishes the functions by an upsurge of PRLR across tissues.

Reproduction: PRL is involved in mammogenesis, lactogenesis and galactopoiesis. Studies have confirmed that disruption of the prolactin gene by knocking out *Prlr* in female mice led to the absence of lobuloalveolar units in the affected animals thereby affecting milk production[56]. Again, PRL promotes progesterone secretion which helps in the luteal preparation of the uterus (corpus luteum formation), although luteolytic characteristics have been observed[57]. It also has an established role in spermatogenesis[58].

Homeostasis: PRL plays a role in establishing the crosstalk between the nervous, immune, and endocrine systems. It is particularly involved in regulating the water/electrolyte balance in the body by reducing sodium and potassium excretion[59, 60]. Rip-Cre neuronal response to PRL was tested in mice and complications of reduced body weight and increased oxygen consumption demonstrated the homeostatic role of PRL in conserving energy by ATPase modulation[61]. Again, hormonal homeostasis is vital in attaining a good functioning immune system[62].

Growth and development: even with an overlap in functions by both PRL and GH, research has been able to demonstrate that there is a distinct variation in functions between them[63]. The role of PRL in growth was assessed in rats which were transplanted with pituitary glands and this led to increased weight in the animals compared to controls, a condition which was correlated to the increased levels of prolactin and not growth hormone[64]. Again, cell culture was able to establish PRL as a key player in cell proliferation. Hepatocytes were cultured in the presence of GH and PRL. There was a marked increase in mitotic figures from the PRL cultures as opposed to the GH which caused a decreased proliferative effect[65]. Several growth factors like the insulin-like growth factor 1 (IGF-1), c-myc, c-jun and others have been found to be inducible by PRL[66-68]. Nevertheless, hyperprolactinemia with an elevation of these transcription factors have been implicated in a subset of breast and prostate cancers, escalating to a state of overstimulation of downstream signaling machinery[69-72]. Contrary to this, underexpression of PRL in *Prl* knockout mice aggravated hepatocellular tumorigenesis with PRL administration rescuing this by preventing activation of hepatocellular carcinoma gene, c-myc[73]. Overall, PRL and PRLR

targeted therapy holds a promise for preventing many related cancers once a well understood course of its action is discovered.

Metabolism and endocrinology: Most endocrine functions corroborate the role of PRL in reproduction. Overexpression studies have been linked to cases of infertility/sterility across both sexes affecting spermatogenesis, limiting mobility of sperms, inhibiting oocyte development and an overall reduced state of breeding tendencies[74, 75]. PRL is known to play a significant role in carbohydrate metabolism with a direct action on pancreatic cells causing insulin secretion. An affiliated study with Dr. Michael Soares lab was done to determine the role of PRLR in glucose homeostasis. Under physiological conditions, maternal organs expand during pregnancy as has been previously demonstrated in our lab[76, 77]. However, conditional disruption of *Prlr* in pancreatic cells of pregnant female mice led to diminished production of β pancreatic islet cells and a decreased islet mass thereby causing insulin inadequacy and eventually disrupting glucose homeostasis (gestational diabetes)[78, 79]. Another function worth mentioning and relevant to this thesis is the known primary role of PRL and its receptor in lipid metabolism. This occurs through lipoprotein lipase and phospholipid biosynthesis activity to reduce accumulation of triglycerides[80]. Increased lipogenesis, fatty acids uptake and decreased β oxidation of fatty acids have been observed in mice from *Prlr* ablation studies using shRNA to silence the gene[80]. Other studies corroborate this with marked hypertrophy of adipocytes being caused by stunted serum levels of PRL and PRLR [81, 82].

Brain function and behavior: it is no surprise that PRL exerts a role in brain function and behavior as it originates from the pituitary gland. Increased secretion of PRL during pregnancy has been seen to induce a sense of responsibility, protection, and development of maternal instincts in mice[83, 84]. This is a contradiction to the observation made in heterozygous mice who do not have both *Prlr* alleles and tend to scatter their pups across the cage or bury them in sawdust without suckling them; but then, after subsequent pregnancies and a surge in PRL over time, they adapt and develop motherly behaviors to nurture their pups[56]. Recent research showed that silencing of the *Prlr* gene disrupted brain derived neurotrophic factor (BDNF) thereby inactivating the JAK/STAT pathway and leading to an exacerbated “chronic mild stress induced depression” in mouse subjects[85].

1.6.2 Extrapituitary PRL

Autocrine secretion of PRL has been determined to be one major source of extrapituitary PRL secretion; the major reason for its many independent and unlinked functions albeit its endocrine and paracrine secretory sources. Transcription and translation of extrapituitary prolactin has been observed in different species and relatively dissimilar to pituitary prolactin[86]. This became salient when hypophysectomized animals still had lactogenic activity with localization of extrapituitary prolactin observed in the decidua, liver, mammary glands and even the brain[87]. Mice subjected to external stimuli and pharmacological factors released extrapituitary PRL as an effect which demonstrated its role as a neurotransmitter in the brain[88]. Extrapituitary PRL is however involved in site specific functions and compliments the activities of pituitary PRL and its functions.

1.6.3 PRLR associated signal transduction pathways

A couple of interconnecting signaling cascades have been associated with the activation of PRLR via the canonical JAK/STAT pathway, the RAS/RAF/MAPK pathway, and other related pathways with an ultimate recruitment of signal transducer and activator of transcription 5 (STAT5)[56, 89-91]. Using a software called the Metacore Pathway Map Creator 2.6.0, we generated a pathway map (**Figure 3**) by feeding the software with genes associated with PRLR signaling and in turn, it provided us feedback with curated data based on known research data and literature.

1.7 PRLR associated phenotypes

1.7.1 *Prlr* homozygous knockout mice (*Prlr*$^{-/-}$)

Prlr$^{-/-}$ female mice have been found to be completely infertile with distorted estrous cycling consistent with irregular mating patterns, reduced ovulation, failure of undergoing pseudopregnancy and an immediate arrest of egg development after fertilization occurs[92, 93]. Due to the inability to bind to PRL, progesterone stimulation is affected which results in failure of embryo implantation. Although exogeneous progesterone can rescue implantation, full term pregnancy is disrupted[94].

Prlr$^{-/-}$ male mice were assessed, and examination revealed normal histology of the genitalia, however, mating with wild-type female mice showed a delay in fertility in approximately 20% of these male mice. PRL administration however rescued this phenotype by modulating the effects of luteinizing hormone on testosterone production as well as spermatogenesis[56, 93, 95]. They are relatively normal compared to their female counterparts albeit marked serum prolactin levels in both genotypes.

1.7.2 *Prlr* heterozygous mice (*Prlr*$^{+/-}$)

Young *Prlr*$^{+/-}$ female mice between 6 to 8 weeks showed a disruption in mammogenesis with a defect in alveolar and ductular development. Studies concluded that one functional allele is not enough for the regulation of PRLR associated functions since decreased levels of PRLR affects mammary epithelial cell proliferation[56, 93]. Due to this, female mice are unable to suckle their young ones causing them to starve to death. However, when left to mature to about 20 weeks, the female mice can produce and nurture pups who survive due to rescue of the phenotype, compensated for by subsequent estrous cycles and pregnancy. This rescue was also seen in the young group when they had their second group of litter. They concluded that two functional alleles are therefore required for PRLR activity.

No discrepancies have been observed in the heterozygous male model.

1.8 Hypothesis and research goals

We hypothesized that PRLR signaling participates in maintaining liver homeostasis and modulating liver disorders. To test this hypothesis, we genetically manipulated *Prlr* to evaluate whether liver health is affected and analyzed the expression and functional states of PRLR in several liver diseases to assess whether PRLR is associated with these diseases.

1.8.1 The role of PRLR signaling in homeostasis

We used the following two experimental conditions to test the hypothesis:

- Deleting the *Prlr* gene specifically in hepatocytes of $Prlr^{flox/flox}$ nonpregnant mice using an adeno-associated serotype 8 (AAV8)-thyroxine binding globulin (TBG)-Cre (AAV8-TBG-Cre) virus.
- Deleting one allele of the *Prlr* gene globally by using pregnant $Prlr^{+/-}$ female mice.

1.8.2 The role of PRLR signaling in diseased conditions

Again, we tested the hypothesis by using the following two liver diseases models:

- BDL-induced extrahepatic cholestasis.
- High fat diet induced-NAFLD.

CHAPTER 2. MATERIALS AND METHODS

2.1 Animal care

All mice were maintained in accordance with protocols reviewed and approved by the Purdue University School of Science Animal Care and Use Committee (IACUC). Animals were provided with standard mouse chow and fresh water ad libitum whilst being housed in a pathogen-free facility at a temperature of 22 ± 1°C, lodged in plastic cages lined with sawdust. Mice were maintained on a 12-hour light/12-hour dark cycle with lights switched on from 7am and turned off at 7pm. Mouse experiments were performed in conformance with the Guide for the Care and Use of Laboratory Animals regulated by National Institute of Health to ensure the humane treatment of mice and to ensure ethical protocols are followed. For the purpose of this thesis, methods and mouse models being used will be categorized according to the designated experimental model.

2.2 Mouse models for homeostasis study

2.2.1 *Prlr* floxed mice (*Prlr*$^{flox/flox}$)

Prlr floxed mice (*Prlr*$^{fl/fl}$) were a gift from Dr. Michael Soares lab in the Department of Pathology and Laboratory Medicine at the University of Kansas Medical Center, Kansas City, USA. Flanking of exon 5 of the *Prlr* gene using LoxP sequences is explained in-depth in the methods section of their paper on pancreatic *Prlr* regulation of maternal glucose homeostasis[78]. The genetic lineage of *Prlr* floxed mice were derived from C57BL/6J mice.

2.2.2 Albumin-cre mice (*Alb-cre*$^{+}$)

B6.Cg-Speer6-$^{ps1Tg(Alb-cre)21Mgn}$/J will hereafter be referred to as Albumin-cre mice for clarity purposes. The homozygous strain of these transgenic mice was obtained from the Jackson Laboratory (Stock No. 003574; Bar Harbor, ME, USA). This transgene expresses cre recombinase under the liver-specific albumin promoter. This is required for the conditional deletion of LoxP flanked *Prlr* gene in hepatocytes and has been proven to be efficient in attaining liver-specific recombination when crossed with liver-specific floxed alleles. [96]. Albumin-cre mice are

maintained as either hemizygotes or homozygotes and are also derived from a lineage of C57BL/6J mice.

2.2.3 Breeding

Prlr$^{fl/fl}$ mice were crossed with *Alb-Cre*$^{+}$ mice which generated hepatocyte-specific *Prlr* conditional mice (*Prlr*$^{Alb\text{-}d/d}$) as shown in **Figure 4**. Wild-type *Prlr* floxed mice were used as controls with *Prlr* homozygous knockout Cre^{+} mice serving as test mice.

2.3 Mouse model for bile duct ligation and high fat diet experiment

24-week-old male mice with a mixed background of C57BL6/129SV were used for the Bile Duct Ligation experiment as well as the High Fat Diet study[97].

2.4 Genotyping

To confirm the genotype of every mouse used, genomic DNA was obtained from 1-2mm of ear snips collected during weaning of litter (21 days after birth), and were ear tagged for identification purposes. DNA was extracted using the Fast DNA extraction reagent (Catalog No. TBS6005) from TriBioScience (Sunnyvale, CA, USA). In a microfuge tube, 40 µL of extraction reagent was added to ear snips and heated on a heat block at 68°C for 7 minutes. It was then vortexed for 5 seconds to disintegrate tissue and 360µL of distilled water was added. It was again vortexed to mix components, spun to bring tissue down to the bottom of the tube for reheating at 95°C for 3 minutes. Samples were then spun at 10,000 rpm for 5 minutes and we performed polymerase chain reaction (PCR) using the supernatant. Amplification of DNA was achieved using TriBioScience Fast Mouse Genotyping System (Catalog No. TBS4033). Specific forward and reverse primers sourced from Integrated DNA Technologies (Coralville, IA, USA) were used to detect the wild-type and mutant alleles (**Table 1**). PCR conditions were optimized at 95°C for 5min; (95°C/min; touchdown at 65°C with 0.5°C decrease per cycle, 68°C/min) for 10 cycles, (95°C/30S; 60°C/ 60S; 72°C/30S) for 28 cycles and 72°C for 5 min in a thermal cycler. A 1.5% gel (for *Prlr*) and 3% gel (for *Alb-cre*) incorporated with 1µL of ethidium bromide was prepared using 3g and 6g of agarose dissolved in 200ml of 1X TAE buffer, respectively. 15µL of DNA was loaded into wells with a 100bp molecular DNA ladder from TriBioScience used as a reference marker (Catalog

number TBS4031). Bands were resolved using electrophoresis; *Prlr*-floxed allele (673bp), *Prlr*-wild allele (487 bp), *Alb-cre* mutant allele (390 bp), *Alb-cre* wild type allele (351bp) shown in **Figure 5** and **Figure 6**. Imaging was done using Bio-Rad's Chemi Doc XRS UV transilluminator.

2.5 Global knock-out of exon 5 and timed pregnancy (pregnancy panel study)

Prlr heterozygous mice ($Prlr^{+/-}$) with a global deletion of exon 5 of the *Prlr* gene were sourced from the Jackson Laboratories (Stock no. 003142)[98]. Appropriate breeding cages were set up between nulliparous heterozygous females and their respective males; with nulliparous wild-type females and males set up as control breeding cages; all between the ages of 10 to 14 weeks. On the next day, the vaginal openings of the female mice were inspected for copulatory plugs and the presence of one was recorded as Gestation Day 1. Pregnant female mice were then separated from their male partners and housed individually. Non-pregnant females belonging to each genotype were also included as controls within each group. Mice were euthanized and livers harvested on designated gestational days (GD 8, GD 10, GD11, GD13, GD15 and GD 18). Litter size ranges from 7 to 10 fetuses.

2.6 Virus injection

20-week-old non-pregnant $Prlr^{fl/fl}$ female mice were injected with AAV8-TBG-Cre virus. The liver specific TBG promoter drives the expression of Cre.(Addgene, AV-8-PV1091). A dose of $1x10^{12}$ genomic viral copies was injected intraperitoneally (ip) per mouse. AAV8-TBG-Null virus (Addgene, AV-8-PV0148) was injected in mice to be used as controls for this experiment. Mice were sacrificed a week after viral injection. Blood and livers were collected for endpoint analysis.

2.7 BDL

Bile duct ligation (BDL) is a procedure performed to induce extrahepatic biliary obstruction and liver fibrosis, eventually causing obstructive jaundice and biliary cirrhosis[99]. The BDL and sham surgical procedures were performed under sterile conditions. To maintain mice under anesthesia, isoflurane inhalation was induced using an isoflurane vaporizer. The common bile duct was ligated by forming two ligatures separated by 2 mm. A cut was made between the two ligatures. Control mice underwent a sham operation (a laparotomy-based procedure consistent with exposure of

abdominal cavity but no ligation of the common bile duct). Post-operative checkups were made to ensure mice were not under any form of distress. Mice were then euthanized at 5-, 10-, 15-, 25-, and 40-days post-surgery and livers collected.

2.8 High fat diet feeding

Mice were given a high fat diet for 16 weeks to induce NAFLD (TD.88137; Harlan Laboratories, Madison, WI) with chow replaced at least once per week[100]. This diet is rich in saturated fatty acids, cholesterol, total fat, and sucrose. After this time frame, mice were euthanized to harvest livers. Another group of mice were maintained on a standard mouse chow to serve as normal diet controls for this experiment.

2.9 Tissue collection and histology

For every experimental model, mice were euthanized at their designated timepoints. Body weights were taken. Livers were harvested and weighed as well. A portion of each liver tissue was fixed in 10% neutral buffered formalin (NBF). This was embedded in paraffin to be sectioned at a thickness of 5µm, hematoxylin and eosin stained, with sectioned slides reserved for other histological analysis. Three different portions of liver were snap frozen in liquid nitrogen to preserve tissue integrity and later stored at -80°C. These were preserved for protein and RNA analysis, with the extra section reserved as backup tissue. Some tissue was also embedded in optimal cutting temperature compound (OCT) (Fisher Scientific,23-730-571) cooled with heptane on dry ice and preserved at -80°C for other required analysis.

2.10 Serum biochemistry

Blood was collected from mice during sacrifice and left to clot at room temperature in a plain tube. Coagulated blood was then centrifuged at 3000rpm for 10 mins to make sure serum was separated from blood cells. Serum was then pipetted into new tubes and sent to Eli Lilly and Company (Indianapolis, IN) for biochemical analysis of liver enzymes and lipids.

2.11 Immunohistochemistry

Formalin-fixed paraffin embedded (FFPE) liver sections were processed for immunostaining to localize proteins in tissue sections. Slides were passed through xylene and increasing grades of alcohol to deparaffinate and rehydrate tissue. Heat-induced antigen retrieval was then performed using citrate buffer (PH 6.0) to break the cross-links formed by formalin fixation to uncover antigenic sites. Slides were then treated with 0.3% hydrogen peroxide for 10 minutes at room temperature to permeabilize tissue. They were then incubated with a blocking solution (goat serum) to reduce non-specific staining. Slides were then incubated with primary antibody against PRLR (50457-T16, HD11SE0515, Rabbit Polyclonal antibody; Sino biological, Beijing, China) ; diluted in 1X DPBS with Ca^{2+} and Mg^{2+} (#114-059-101, Quality Biological, Inc.) (1:1000 ratio) and incubated at 4°C overnight for maximal binding. Biotinylated secondary antibody against PRLR (111-065-144, Lot No. 133440; Biotin-SP Conjugated Affinipure Goat Anti-Rabbit IgG (H+L) Jackson Immuno Research Labs) was diluted with 1X DPBS with Ca^{2+} and Mg^{2+} (1:200) and added to slides with incubation for an hour. Vectastain ABC peroxidase reagent (PK-6100, Vector Laboratories, CA, USA) were added to slides for 30 minutes to enhance the binding of avidin to biotin. Detection of PRLR localization in tissues was then performed using DAB substrate as a chromogen. Counterstaining is done with hematoxylin (Leica; 3801575) for 1 minute. Slides are dehydrated with increasing grades of alcohol and xylene and mounted using Vectamount AQ mounting medium. (#H-5501, Vector Laboratories, Inc.)

2.12 Oil red o staining

10µm of cryo-embedded liver sections were also processed for Oil red o staining (1024190250, Sigma-Aldrich, St. Louis, MO, USA) to visualize intracellular fat droplets according to manufacturer's instructions.

2.13 Western blotting

Liver sections were homogenized using a mixture of T-PER Tissue Protein Extraction Reagent (78510, Thermo Scientific) and Pierce, Halt Protease & Phosphatase Inhibitor Single-Use Cocktail, EDTA-free (No. 78443), according to liver weights. 10µL volume of diluted lysates were incubated with 150µL of Pierce 660nm Protein assay reagent (Thermo Scientific No. 1861426)

and protein concentrations were measured using the Nanodrop 2000 spectrophotometer from Thermo Scientific. 10µg/15µL of loading samples were loaded into wells of precast gels (Invitrogen NP0323BOX; Thermo Fisher Scientific) for separation by polyacrylamide gel electrophoresis. Proteins were then transferred onto polyvinylidene difluoride (PVDF) membranes by passing electrical current through the gel and membrane sandwich. Transfer was confirmed by Ponceau S staining. Membranes were blocked with either non-fat dry milk or bovine serum albumin (BP-1605-100; Thermo Fisher Scientific). Primary and HRP-coupled secondary antibodies were added to membranes and incubated whilst on a shaker (**Table 2**). Chemiluminescent substrate was then added for band detection (Super Signal West Pico PLUS, Ref: 34577; Thermo Scientific, USA). Membranes were then imaged using ImageQuant LAS 4000 mini to reveal protein bands. Densitometric analysis was done using ImageJ software.

2.14 In-situ hybridization

In-situ hybridization was done using the RNAscope 2.5 HD Assay-Brown Kit (Catalog no. 322300; Advanced Cell Diagnostics-ACD). This was performed following manufacturer's guidelines and protocols. Probes used for PRLR was Mm-*Prlr*; 430791; Advanced Cell Diagnostics. A negative control probe *DapB* (310043) and a positive control probe *Ppib* (313911) were used as experimental quality controls.

2.15 RNA isolation

Four biological replicates of liver sections from each group of cre and null virus deletion were selected, and total RNA was isolated using the Qiagen RNeasy Plus Mini Kit (catalog number 74104). High yields of total RNA were extracted by following the manufacturer's protocol. Ribonucleic acid concentration was measured using Nanodrop 2000 Spectrophotometer. 5µg of loading samples were prepared using the RNA sample loading buffer containing ethidium bromide (R4268, Sigma-Aldrich) and the quality of RNA samples were assessed by running an RNA integrity gel electrophoresis. Bands were resolved by imaging using the Bio-Rad Chemi-Doc XRS imaging device. RNA samples were stored at -80°C for future usage.

2.16 Quantitative real-time polymerase chain reaction (qRT -PCR)

Using the Verso cDNA kit from Thermo Fisher Scientific (AB1453/B), Complementary DNA (cDNA) was synthesized from 1µg of total RNA. 20µL of this was diluted with 60µL of molecular grade water to achieve a 1 in 4 dilution. qRT-PCR was then performed using 2X TaqMan qPCR Super Mix from TriBioScience (TBS4002) using probes specific to genes, sourced from Applied Biosystems; Thermo Scientific (**Table 3**). This reaction took place at 50°C for 2 min for uracil N-glycosylase (UNG) incubation, 95°C for 10 minutes for polymerase activation and 40 cycles of amplification at 95°C/15 secs; 60°C for 1 min. Relative gene expression was presented as fold change by normalization to 18S rRNA (housekeeping gene) transcript levels and analyzed using the comparative Cycle threshold (C_T) method; $\Delta\Delta C_T$.

2.17 RNA sequencing

RNA samples were diluted to 500ng/µL, and sequencing was performed and analyzed by BGI Genomics (BGI Americas Cooperation, IL,USA). RNA concentration was measured at the BGI labs using Agilent 2100 Bioanalyzer as well as assessment of RNA quality (23S/18S and 23S/16S). Overall, all samples passed quality control with an RNA integrity number (RIN) ≥ 8. A strand-specific transcriptomic cDNA library was constructed from total RNA samples and assessed with Agilent 2100 Bioanalyzer as well. Libraries were clustered, amplified and sequenced using DNBSEQ sequencing system. Phred quality score (Q score) was used to measure quality of sequencing. Reads were filtered using the BGISEQ platform. Reads of low quality, connector contamination, and excessively high levels of unknown bases were removed before analysis of results (**Figure 7**). Clean reads were then mapped onto the mouse genome using HISAT alignment program. Clean reads were also aligned to the reference genes using Bowtie2 (v2.2.5) and RSEM to calculate the gene expression level of each sample. Differential gene expression was analyzed using DESeq2 with Q values < 0.05. Other data analysis and pathway analysis were performed using BGI's Dr. Tom multi-omics data analysis, visualization and interpretation software.

2.18 Statistical analysis

Statistical analyses were performed depending on the variables factored for during analysis. Unpaired students t-test or one-way analysis of variance (ANOVA) and two-way ANOVA were

employed using Microsoft Excel. Data are shown as mean ± standard error of the mean (SEM), with significant differences defined when $P \leq 0.05$.

CHAPTER 3. RESULTS

3.1 The role of PRLR in maintaining homeostasis

3.1.1 AAV8-TBG-CRE effectively deletes *Prlr* in hepatocytes of mice

We hypothesized that PRLR plays a role in maintaining a state of equilibrium in the liver. To test this, we induced a conditional deletion of *Prlr* in hepatocytes of mice to create a loss-of-function mutation. This was to highlight the effect of its absence on the signaling pathways involved in synchronization of liver homeostasis. We achieved this by injecting mice with AAV8-TBG-Cre virus. Control mice were injected with the null virus vector, AAV8-TBG-Null virus. On the day of sacrifice, gravimetric measurements of total body and liver weights were recorded, and analysis showed no significant variation in average liver-to-body weight ratio between both groups (**Figure 8**). This result indicates that PRLR is not required for the liver to maintain its size. Western blot analysis however showed the disappearance of long and short isoforms of PRLR after deletion by cre-virus; as compared to the null controls (**Figure 9**). This indicates the high efficiency of the cre vector in deleting the *Prlr* gene in hepatocytes. Mice from the cre deletion group will hereafter be classified as *Prlr* knockout mice ($Prlr^{-/-}$).

3.1.2 Conditional deletion of *Prlr* in the liver results in dysregulation of certain metabolic functions

Using serum, we assessed the liver function enzymes and metabolites involved in the daily metabolic functioning of the liver by biochemical and serological assays. Electrolyte balance was relatively the same in both genotypes (data for Na^+, K^+ and Cl^- not shown), however a significant increase in blood urea nitrogen levels was recorded. The elevation of circulating levels of urea highlights the inefficient excretion of this substance which is a waste product of protein deamination by the liver. Serum ALT and AST levels remained unaltered by knockout of *Prlr*, as well as other liver enzymes. However, a slight elevation in triglyceride and glucose levels was observed in knockout mice (**Figure 11**). Consistent with previous studies in which both long and short isoforms of *Prlr* were silenced using a short hairpin RNA (shRNA)[80], the assessment of gross liver morphology and immunohistochemical analysis revealed some moderate level of hepatic steatosis. Comparison of immunostaining between knockout and control livers showed

uniform expression of PRLR in wild-type mice with marked reduction in knockouts (**Figure 12**). These observations indicate that PRLR is likely involved in some homeostatic functions like the urea cycle.

3.1.3 Evaluation of *Prlr* mRNA distribution in both male and female murine hepatocytes

Using in-situ hybridization (ISH), we assessed the distribution of *Prlr* mRNA in the livers of $Prlr^{fl/fl}$ mice. To determine if there was any gender-bias among both sexes, we characterized the expression of *Prlr* mRNA in male mice as well as in the distinct stages of estrous cycle in female mice. The estrous cycle is a representation of the recurring cyclical ovarian changes that occurs in females and lasts between 18 to 24 days. It involves changes in the uterine lining and ovulation assessed by cytological analysis of vaginal specimen collected from female mice. Mice were then classified as pro-estrus, estrus, diestrus and metestrus and in-situ staining was done using probes alongside the RNAscope brown kit from ACD. Results showed that both female and male mice had an abundant expression of *Prlr* mRNA in hepatocytes; uniformly distributed across all three zones. However, more pronounced expression was observed in female mice (shown by the brown deposits of mRNA) (**Figure 13**).

3.1.4 Dysregulation of JAK2/STAT5 pathway after deletion of *Prlr* in mouse hepatocytes

The recruitment of STAT5 by PRLR via the JAK/STAT signaling cascade has been reported by many publications[101, 102]. To investigate the effect of hepatocyte-specific *Prlr* knockout on this canonical pathway, we sought to explore with a focus on the signaling pathway proteins. As expected, densitometric analysis of western blot bands revealed an overt depletion or loss of both 95kDa and 45kDa isoforms of PRLR in cre-virus treated livers. With this confirmation, we then assessed proteins downstream of PRLR signaling. T-STAT5A and p-STAT3 exhibited PRLR-dependent changes with a marked decline in expression seen in knockout livers; accounting for an approximate two-fold decrease. Phosphorylation of these proteins are achieved by phosphorylation of Janus kinases in response to binding of ligands to the PRLR. This in turn causes phosphorylation of STAT3 which in turn dimerizes and phosphorylates STAT5. Phosphorylation of both STAT3 and STAT5A are crucial for nuclear translocation and activation of transcription factors responsible for cell growth and immune function of the liver[103]. The abrupt decline in p-STAT3

however explains the downregulation of T-STAT5A expression and thereafter its unphosphorylated state. Nonetheless, T-STAT5B was unaffected. (**Figure 9** and **Figure 10**). DMBT1 (Deleted in malignant brain tumors 1) is highly involved in liver repair and maintenance of homeostasis. Analysis of its protein expression levels revealed a marked reduction in knockout mice as compared to wild-type mice, which also suggests dysregulation of homeostatic functionalities.

3.1.5 RNA sequencing analysis reveals PRLR-dependent transcriptomics in mouse liver

In order to profile PRLR target genes, we compared transcriptomics of null-virus livers to cre-virus livers deficient in *Prlr* by performing RNA-seq. The correlation of gene expression between all samples were validated by calculation of the Pearson correlation coefficient and analyzed in the form of a heatmap. With a massive repression in PRLR, analysis with the Metacore pathway analysis software applying a false discovery rate (FDR) of 0.05 revealed as low as 133 differentially expressed genes (DEG's), reflecting varied upregulation and downregulation of the profiled genes. Out of the 133 genes assayed, only 31 genes were downregulated due to loss of *Prlr* whilst 102 were upregulated in this respect. KEGG pathway analysis suggests the involvement of these genes in many crucial biological processes and subcategorized into cellular processes, metabolism, organismal systems and environmental information processing. Further analysis with subclassifications of these processes is shown in **Figure 14**. Predictably, this suggests most genes were associated with cytokine-cytokine receptor signaling pathway, prolactin receptor signaling pathway, JAK/STAT signaling pathway, PI3K/AKT signaling pathway, among others which are top pathways modulated by *Prlr*. This shows the involvement of PRLR in regulating a spectrum of genes; explicitly or implicitly engaged in numerous functions required for modulating liver homeostasis.

3.1.6 Hepatocyte-specific knockout of *Prlr* leads to activation of certain key functional proteins in hepatocytes

With the results generated from RNA-seq analysis, we sought to explore some of the genes being regulated by the *Prlr* gene. Key genes such as *Acta2, Actg2, Cxcl13, Glut4, Ntrk2, Marco, Pnpla3* and *Cyp2b13* were quantified and analyzed. To validate the RNA-seq data, we quantified mRNA

levels of these genes using qRT-PCR primers which spans across the exons of these genes in knockout and wild-type mouse livers. Results showed that loss of *Prlr* led to approximately 2.5-fold decrease in *Cyp2b13* (Cytochrome P450, family 2, subfamily b, polypeptide 13), a crucial liver and biliary gene involved in response to stimuli, lipid metabolic processes and xenobiotic metabolism. Contrary to this, a robust 7-fold induction of *Marco* mRNA was expressed after deletion of *Prlr* in knockout livers. *Marco* (macrophage receptor with collagenous structure), a pattern recognition receptor with a role in inflammation is associated with reduced response to a ligand within a cell. Also consistent with inflammation is a 6-fold increase of an immune response chemokine, *Cxcl13*. Significant mRNA expression of a family of actin proteins such as *Acta2* and *Actg2* were also consistent with deletion of *Prlr* in knockout livers; both accounting for an approximate 3-fold increase (**Figure 15**).

3.2 One functional *Prlr* allele may be sufficient for PRLR activity in the maternal liver

To test the role of PRLR in the liver during pregnancy, we used *Prlr* heterozygous ($Prlr^{+/-}$) female mice due to the infertile nature of homozygous female mice. *Prlr* wild-type ($Prlr^{+/+}$) females were used as control mice. Female mice were crossed with male counterparts to induce a state of pregnancy validated by the presence of copulatory plugs. Female mice who were confirmed to be pregnant were housed separately from males and liver samples were collected over the stipulated gestational days mentioned in the methods section. The liver weights were recorded, and as previously demonstrated in our lab, maternal liver adaptations to pregnancy induced an overt doubling in the size of livers in pregnant mice[76]. However, heterozygous female mice had a slightly higher liver-to-body weight ratio as compares to their wild-type counterparts; except for the eighth-day of pregnancy where wild-type mice were seen to have recorded a higher ratio (**Figure 16**). Western blot analysis of PRLR (**Figure 17**) revealed that in the early stages of pregnancy, heterozygous female mice exhibited a significant decrease in PRLR-S which was compensated for, by day 15 of the second-half of gestation. This compensation on day 15 was also observed in PRLR-L although it was overtly reduced throughout the duration of pregnancy. However, most key players of the JAK/STAT pathway were not affected during pregnancy except for p-STAT 3. Its expression was seemingly relative to wild-type in the early stages of pregnancy however on day 11, there seemed to be another compensation in heterozygous female mice which

reduced towards the second half of pregnancy. The unperturbed nature of the JAK/STAT proteins may suggest that during pregnancy, PRLR inefficiency may be rescued or compensated for. It may also imply that one *Prlr* allele is sufficient to synchronize the JAK/STAT signaling pathway or regulation of this pathway by other transcriptional factors present in the liver. DMBT1, was however reduced in the early stages of pregnancy in heterozygotes as compared to wild-type but an overt increase occurred mid-gestation and on day 18 in heterozygotes.

3.3 The role of PRLR in pathological conditions

To test the role of PRLR in diseased conditions, we studied its role under two pathological conditions, NAFLD induced by high fat diet and extrahepatic cholestasis induced by bile duct ligation.

3.4 NAFLD induced by high fat diet

3.4.1 Fatty liver disease completely inactivates the short isoform of PRLR (PRLR-S)

To determine if PRLR plays a role in lipid metabolism, we induced NAFLD by feeding mice with a diet saturated in fats for four months as described in the methods section. Control mice were fed with standard chow. Mice fed a high fat diet exhibited an enlarged liver [100] with massive infiltration of hepatic fat when hematoxylin and eosin staining was done to reveal liver histology (**Figure 18**). To further substantiate induction of a fatty liver state, we measured lipid levels which revealed massive accumulation of triglycerides, free fatty acids and cholesterol in mice on high fat diet relative to the mice fed with normal chow[100]. We further stained slides to visualize intracellular adipocytes and lipid droplets using oil red o staining (**Figure 19**). Western blot analysis of the expression of PRLR protein in biological replicates however revealed some striking results; the short isoform of PRLR (PRLR-S) was completely depleted in mice fed with high fat diet. Nonetheless, no relative changes were seen in the long isoform of PRLR (PRLR-L) as compared to the normal chow group of mice (**Figure 20**). Densitometric analysis corroborates marked significance in the loss of this short isoform in mice with NAFLD (**Figure 21**). Together, these findings suggest that PRLR-S is highly involved and may be the utmost regulator of lipid metabolism in the liver.

3.4.2 Downstream signaling of PRLR in the liver may be modulated by PRLR-L

We further assessed the signaling pathway proteins associated with PRLR using western blotting analysis. The data (**Figure 20** and **Figure 21**) reveals significant reduction in T-STAT3 of diseased mice however, phosphorylation of this signaling protein was observed. Notably, p-STAT3 was highly and significantly expressed in fatty liver states as compared to normal liver states. Contrary to the effect seen in p-STAT3, a significant reduction was observed in both expression levels of T-STAT5A and B. Altogether, phosphorylation of STAT5 proteins (p-STAT5) was reduced in fatty livers albeit not a significant effect. A comprehensive look at this data suggests that the long isoform of PRLR may be responsible for modulating downstream signaling pathways; however, requires some support from PRLR-S. DMBT1 which is involved in regeneration of liver and metabolism of proteins was highly depleted in fatty livers relative to mice with healthy livers; although analysis showed no significance. This effect also suggests a correlation between PRLR-S and DMBT-1. PRLR-S has been determined to be widely abundant in liver as compared to PRLR-L[73], however these findings suggest that the PRLR downstream signaling pathway could be modulated mainly by the long isoform of PRLR as it serves as the major receptor in JAK/STAT signaling[104].

3.5 Extrahepatic cholestasis induced by BDL

3.5.1 PRLR-S may play a protective role during the progression of extrahepatic cholestasis in mouse livers

To elucidate the role PRLR plays in bile acid homeostasis, we induced extrahepatic cholestasis also known as obstructive jaundice which progresses into liver fibrosis. Generally, bile acids play a role in lipid catabolism, absorption, and turnover however, a cholestatic liver fibrosis state accounts for disruption of the flow of bile; hence its accumulation in hepatocytes and blood serum and consequently its inability to breakdown fats. BDL surgeries were performed on three biological replicates for each time point; by making two different ligatures on the common bile duct separated 2mm apart and sacrificed on 5-, 15- and 40-days post BDL. Another group of mice which underwent a sham procedure served as controls for this model. Liver fibrosis was confirmed using Sirius staining (**Figure 22**). Western blot analysis (**Figure 24** and **Figure 25**) revealed an overt significant decline of PRLR-L relative to the sham at all timepoints of BDL; worsening as

the days progressed. A similar phenomenon was observed in PRLR-S however on day 15, its expression levels increased. This data reveals the disruption in PRLR expression during pathogenic states. DMBT1 which is required for epithelial cell differentiation was absent in sham controls however as cholestasis advanced, there was a colossal upregulation in its expression which suggests its induction by BDL. Overall, the data suggests that BDL-induced cholestatic liver fibrosis interferes with PRLR expression levels which may lead to the disruption of bile acid homeostasis and upregulation of DMBT1; however, the upregulation of PRLR-S at day 15 suggests it may have an involvement during the pathogenesis of cholestatic liver fibrosis.

3.5.2 Hepatocytes highly activates PRLR signaling pathway proteins and NQO1 to adapt to cholestasis

To further elucidate the regulation of PRLR downstream signaling during cholestasis, we investigated protein expression levels of the pathway proteins and observed that as cholestasis progressed, there was a continuous significant upregulation of p-STAT3, T-STAT3, T-STAT 5A and T-STAT5B compared to sham controls. Surprisingly, the definitive player, p-STAT5 which will account for nuclear translocation slightly increased after BDL but remained relatively unchanged at all timepoints with no significance as compared to the sham (**Figure 24** and **Figure 25**). This implies that activation of STAT proteins may be induced by BDL progression to help counteract the damage caused by disruption in bile acid homeostasis. An ongoing lab project on BDL (manuscript under review), involving *Nrf2* wildtype and knockout mice was used to assess hepatic Nrf2 function (required for redox homeostasis). We evaluated its target gene *NQO1* which has been found to be directly regulated by *Nrf2* in BDL-associated cholestatic fibrosis[105]. We found that NQO1 expression increased as cholestasis advanced, relative to the sham (**Figure 23**) (expression data not shown). Together, this data suggests that hepatocytes respond to cholestasis by highly activating pathway signaling proteins and other key proteins to thwart the oxidative stress induced by cholestatic damage.

CHAPTER 4. DISCUSSION

4.1 Deletion of *Prlr* dampens PRLR signaling pathway with a disruption in homeostasis

The abundant and homogeneous expression of PRLR in the liver has been a fascinating occurrence which requires a lot of exploration to elucidate its mechanism of action. In this study, we have been able to characterize prolactin receptor expression and activity in the liver of mice under physiological and pathological conditions with our findings postulating a dampening in PRLR signaling when the gene is disrupted.

Using an infallible approach of inducing loss-of-function mutation in which *Prlr* was inactivated by adenoviruses, we have been able to demonstrate that absence of *Prlr* led to dysregulation of the urea cycle. Knockout mice produced copious amounts of urea from deamination of amino acids in the liver, reflected by decreased levels of globulin. However, excretion of this toxic waste substance by the kidneys was impaired which led to its accumulation in the blood. To further confirm this, an index used to assess acute renal failure by measuring blood urea nitrogen to creatinine (BUN:CREA) ratio was calculated for, which accounted for values above the normal range (data not shown). Decreased creatinine levels plus uremia is coherent with a study whereby hyperprolactinemia mediated reduced osmolar clearance in man[106]. This implies a communication between the liver and kidney to systematically coordinate homeostatic functions. Although we recorded no significant variation in liver-to-body weight ratio among both wild-type and knockout mice, congruent with the loss of *Prlr* was a disruption in triglyceride homeostasis exhibited by an increase in triglycerides; leading to moderate levels of hepatic steatosis and dyslipidemia. This indicates some interference in lipid metabolism consistent with previous reports by Shao et al whereby depleting hepatic PRLR aggravated liver steatosis with more severity in males[80]. This also confirms results from studies which found a correlation between hyperprolactinemia and hyperlipidemia[107, 108]. The above observations however ignited an interest in investigating the downstream signaling pathway modulated by PRLR and if disruption of any of the key players caused an imbalance in homeostasis. We performed western blot analysis of proteins involved in the JAK/STAT pathway which has been determined by many publications as the canonical pathway regulated by PRLR[101, 102]. The typical function of phosphorylated proteins in this pathway is to ultimately activate p-STAT5 which translocates to the nucleus to

effect cell survival and progression of the cell cycle. Notably, all STAT proteins except for T-STAT5B were relatively reduced in knockouts as compared to their controls; with significant decline in p-STAT3 and T-STAT5A. At this point, we cannot explain the rather increased level of T-STAT5B however, a newly designed computational model to make a distinction between STAT5A and STAT5B predicts a higher nuclear translocation rate of STAT5B as compared to STAT5A in response to prolactin[102]. Based on this model, we postulate that the accumulation of prolactin due to knocking out of *Prlr* may lead to faster homodimerization of STAT5B and its translocation to the nucleus; which could account for the phosphorylation of p-STAT5 observed in knockout mice. Although not statistically significant, DMBT1, an anti-inflammatory gene involved in terminal differentiation of epithelial cells and embryonic stem cell was highly reduced in knockout mice. Some studies have reported the induced expression of DMBT1 to be dependent on p38 and STAT3 signaling[109]. Although we have observed STAT3 reduction being consistent with a decline in DMBT1, we were not able to show a direct correlation in this study. Nonetheless, we are interested in exploring this in future studies.

As analyzed by RNA sequencing, PRLR modulates the expression of 133 target genes in the liver (102 upregulated, 31 downregulated; $p \leq 0.05$). This suggests PRLR generally activates rather than suppresses transcriptional responses to its signaling pathway. Another point worth mentioning is the fact that a high number of upregulated genes belong to the actin family of proteins; a major component of cytoskeleton. KEGG pathway analysis predicted the involvement of *Prlr* gene in many signaling cascades required for equilibrium in the liver; mainly cytokine-cytokine receptor interaction, vascular smooth muscle contraction (which explains upregulation of actins), prolactin receptor signaling pathway, JAK/STAT signaling pathway, among others. This transcriptomic revelation affirms the prediction of the pathway map analysis in **Figure 3** which asserts the role of PRLR downstream signaling in cytoskeletal remodeling.

To verify PRLR-dependent transcriptomics divulged by RNA sequencing analysis, we carefully selected some of the topmost upregulated and downregulated genes and performed quantitative real-time polymerase chain reaction (qRT-PCR) analysis. Out of a large group of actin proteins analyzed, *Acta2* and *Actg2* exhibited a significant three-fold increase in knockout mice. Noteworthy is the robust expression of *Marco* and *Cxcl13* mRNA levels; yet again, another indicator of disarranged homeostasis is seen when *Cyp2b13* levels are downregulated. This is a

cytochrome P450 polypeptide required for drug metabolism, lipid metabolism and metabolism of numerous compounds in the liver; acting as an oxidoreductase agent[110]. An in-vitro CYP450 inhibition study showed that decreased levels of prolactin hormone and its receptor caused a decline in metabolic activity of CYP2D2 in rats[111], however our results reveal a PRLR/CYP2B13 axis in mice. Future insights into this will incorporate the relationship between PRLR and the promoters of CYP2B13 to determine any PRLR-dependent activity.

Due to the ubiquitous expression of PRLR, we cannot exclude the possibility that other signaling cascades or proteins may contribute to/or account for homeostatic roles in the liver. Overall, our study postulates that loss of PRLR causes a distortion in maintenance of homeostatic balance in the body.

4.2 Maternal PRLR activity in heterozygotes is rescued during the second half of pregnancy

We previously studied maternal adaptations to pregnancy which showed that hepatomegaly in pregnant female mice is a physiological response to the increased metabolic demands in the body[76]. In this context, we aimed at assessing the in vivo homeostatic role of PRLR during pregnancy; made possible by using mice heterozygous for the global *Prlr*-null mutation. *Prlr* wild-type mice having two functional alleles served as controls. Generally, we observed a slightly higher liver weight in heterozygotes as compared to wild-type mice and this may be due to the profound hepatic adjustment of hepatocytes in order to meet the required metabolic demands of mice with only one functional allele. Assessment of PRLR protein expression revealed a steady decline of PRLR in heterozygotes relative to wild-type; particularly in PRLR-S during the first half of pregnancy. At mid-gestation, both in the long and short isoforms, relative PRLR expression was highly compensated for, which could be due to accumulation and overt release of prolactin during gestation. Same was seen for DMBT1 which had a spike around mid-gestation and day 18 of pregnancy. Considering its role in epithelial cell proliferation, this compensation correlates with the increased liver size in heterozygotes as compared to wildtype controls; strongly suggesting an increased hepatic induction of metabolic adaptation in heterozygotes. Evidence supports the notion that during breeding, pups from heterozygous female mice tend to die between few hours to a day after parturition[56]. This phenomenon which we also encountered has been proven to be due to the inability of heterozygotes to suckle their young ones as a result of defects in alveolar

development. This led to Bole-Feysot et al reporting that two functional *Prlr* alleles are required for PRLR activity in lactation. However, subsequent pregnancies always resulted in surviving pups (also recorded by this group). We speculate that the compensation seen during the first pregnancy may be responsible for the stimulation of further estrous cycles to account for the fully functional effect of PRLR seen in subsequent pregnancies. Yet again, they reported that sisters of these heterozygotes who were left to grow until 20 weeks before breeding had surviving pups. Considering that none of the downstream signaling pathway players were severed in heterozygotes combined with compensatory effects recorded during the second half of pregnancy, we conclude that someway somehow, the compensation rescues PRLR activity which makes one functional allele sufficient for PRLR activity.

4.3 PRLR-S may be the major modulator in lipid metabolism

With previous sex-dependent studies demonstrating an aggravated NAFLD diseased state in males than in females, we sought to explore the effects of inducing fatty liver disease in males to assess its effects on PRLR. We however made some striking discoveries. For the first time ever, we report complete inactivation of the short isoform of PRLR in NAFLD mice. The long isoform of PRLR however remained intact with seemingly relative levels as the controls. This led to us questioning if PRLR-S is the major regulator of lipid metabolism as an induced state of dyslipidemia is associated with its absence. At this juncture, we have not been able to answer this question. However, with a speculated involvement of PRLR in lipid metabolism, complete depletion of the protein during a fatty liver state corroborates the fact that PRLR-S is the dominant isoform of PRLR in the liver [73]. A look into the JAK/STAT signaling in these mice show significantly reduced expression levels of STAT proteins except for p-STAT3 whose expression levels were remarkable in NAFLD mice. Nonetheless, there was phosphorylation of STAT5 proteins, although reduced than levels seen in mice fed with normal diet; showing dysregulation in homeostasis. This implies that PRLR-L may be sufficient to modulate downstream signaling of PRLR to an extent but requires PRLR-S for maximal transcriptional effects. This is in concordance with some cell culture studies which showed that PRLR-S mediates liver signaling in differentiated hepatocytes[73]. Contrarily, this disputes previous studies which believe PRLR-S has no significant role in JAK/STAT signaling but then again, they experimented in rats whilst we used

mice[112]. With our current in vivo analysis, we support the in-vitro work done by Hartwell et al to postulate that PRLR-S may support PRLR-L for maximal modulation of JAK/STAT signaling. Again, due to the marked reduction of DMBT-1 in NAFLD mice, we also speculate an association between DMBT-1 and PRLR-S. Considering that absence of PRLR-S leads to a cutback in the reparative function of DMBT-1 protein post injury (fatty liver state) to the liver, there may be an associated connection between the two; although previous research suggests DMBT-1 plays a minor role in hepatic steatosis[113]. For a long time, the exact role of PRLR-S has not been elucidated. Nonetheless, we are currently devising an efficient strategy to study in its entirety, the exact involvement of PRLR-S in lipid metabolism. We aim at using loss/gain-of-function mutation models incorporated with CRISPR/Cas9 mutations or short hairpin to block PRLR-S in order to investigate its role. Ultimately, we also aim to understand the gender-dependent bias in this phenomenon and determine why it affects males more than females.

4.4 PRLR may be associated with the progression of extrahepatic cholestasis.

Liver fibrosis and extrahepatic cholestasis induced by BDL took a toll on PRLR protein expression. As BDL progressed, mouse livers were generally seen to have a decline in PRLR protein levels. However, the switch seen on day 15 poses a lot of questions, due to the expression patterns of PRLR-S in response to BDL. First of all, when we analyzed the STAT proteins, a trend was observed; in that almost all of these proteins were increased, with marked significant upregulation in total STAT5A and B seen on the said day 15. Nonetheless, p-STAT5 which culminates the downstream signaling cascade was observed to increase due to induction of BDL; although not significantly expressed but remained relatively unchanged. With the occurrences seen in this model (significant expression of PRLR-S and STAT proteins), we believe the upregulation of STAT proteins is an oxidoreductive phenomenon or protective response to cholestasis rather than the canonical signaling stimulation to effect cell proliferation. This is however consistent with previous research, which shows that activation of STAT proteins; both total and phosphorylated may serve as an inflammatory feedback mechanism to help counteract the dysregulation of homeostatic proteins [114]. Also supporting this claim is the virtually absent levels of DMBT1 expression in the sham controls and its steady increment during BDL, which massively peaks on day 40 post BDL. This validates its role in tissue repair as its expression increases as cholestasis

advanced to salvage the fibrotic nature of the liver[115]. NAD(P)H Quinone Dehydrogenase (NQO1), which is transcriptionally activated by NRF2 has been shown to be highly involved in the oxidative stress pathway; serving as a quinone reductase during some pathological states[116]. Hepatic overexpression of NQO1 was also accompanied by induction of BDL; increasing with BDL progression. This suggests that antioxidant genes are activated in response to BDL through NRF2. This is validated by research in our lab and other labs [105] using *Nrf2* wild-type and knockout mice. A complete absence of NQO1 in *Nrf2* knockout mice confirm it to be a direct target for NRF2 during bile duct ligation (manuscript under review). Overall, our data suggests that BDL-induced obstructive cholestatic fibrosis causes a disruption in bile acid homeostasis as well as PRLR expression; thereby inducing an upregulation of antioxidant genes and STAT proteins to counter the oxidative damage; implying a potential link between PRLR signaling and NRF2 signaling.

4.5 Future research approaches

Considering the exploratory nature of this study, this research has served as a foundation to divulge into many specific aspects of PRLR activation and modulation. Overall, our study suggests a disruption in *Prlr* gene causes dysregulation of many physiological processes and a critical role for PRLR in maintaining homeostasis. Future studies will focus on elucidating specific ligands responsible for activating Prlr/JAKSTAT pathway by eliminating growth hormone and placental lactogen. Specific targets we aspire to focus on includes finding out if PRLR is the key regulator transducing mitogenic signaling which drives hepatocyte proliferation during liver regeneration induced by partial hepatectomy. We aim to incorporate overexpression analysis using ovine prolactin and hepatocyte proliferation assessment using BrdU and Ki67 positive hepatocytes. Another target is using RNAi or mRNA approaches to either induce blockade or restoration of PRLR-S expression to determine its specific role in the formation of hepatic fatty liver disease or steatosis. A breakthrough in this will help develop therapeutic drug targets to effectively intervene in NAFLD.

FIGURES

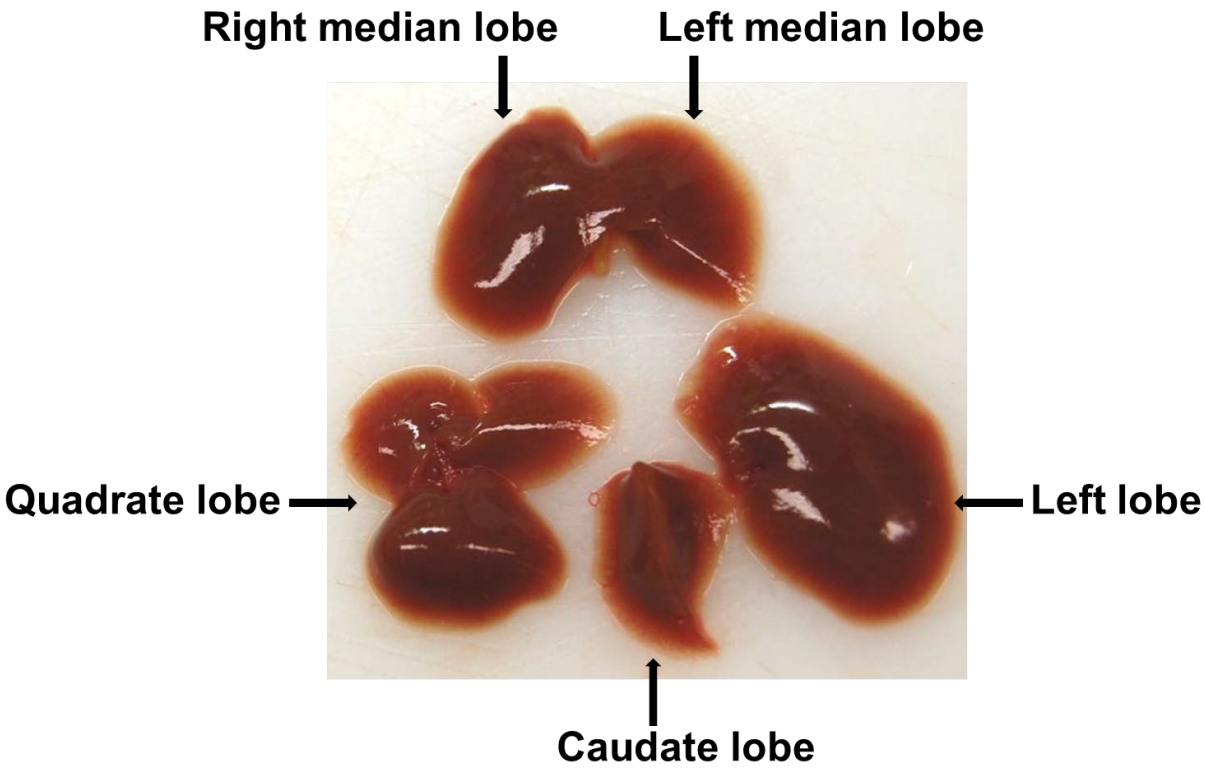

Figure 1. Lobes of the liver

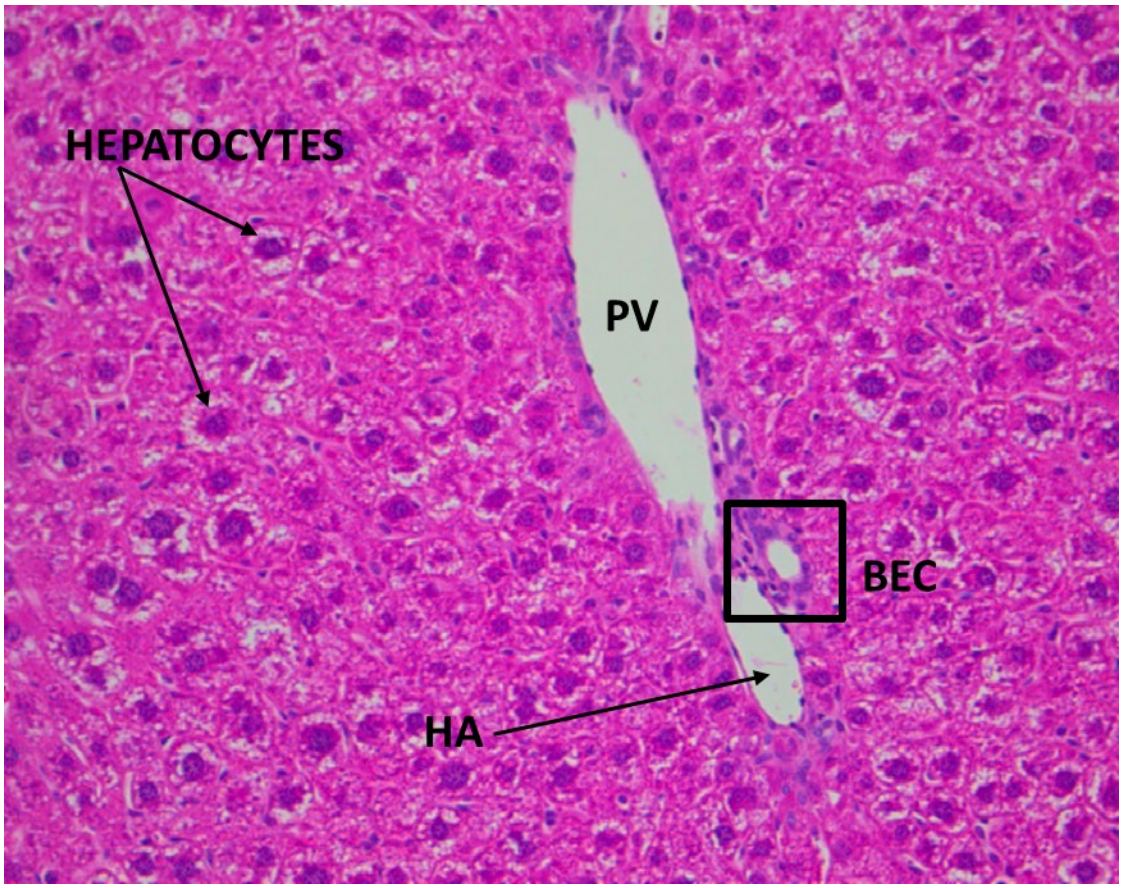

Figure 2. Hematoxylin and eosin staining of liver- reveals hepatocytes containing nuclei. PV- portal vein, BEC- biliary epithelial cells surrounding the bile duct, HA-hepatic artery. Together, the portal vein, bile duct and hepatic artery make up the portal triad of the liver.

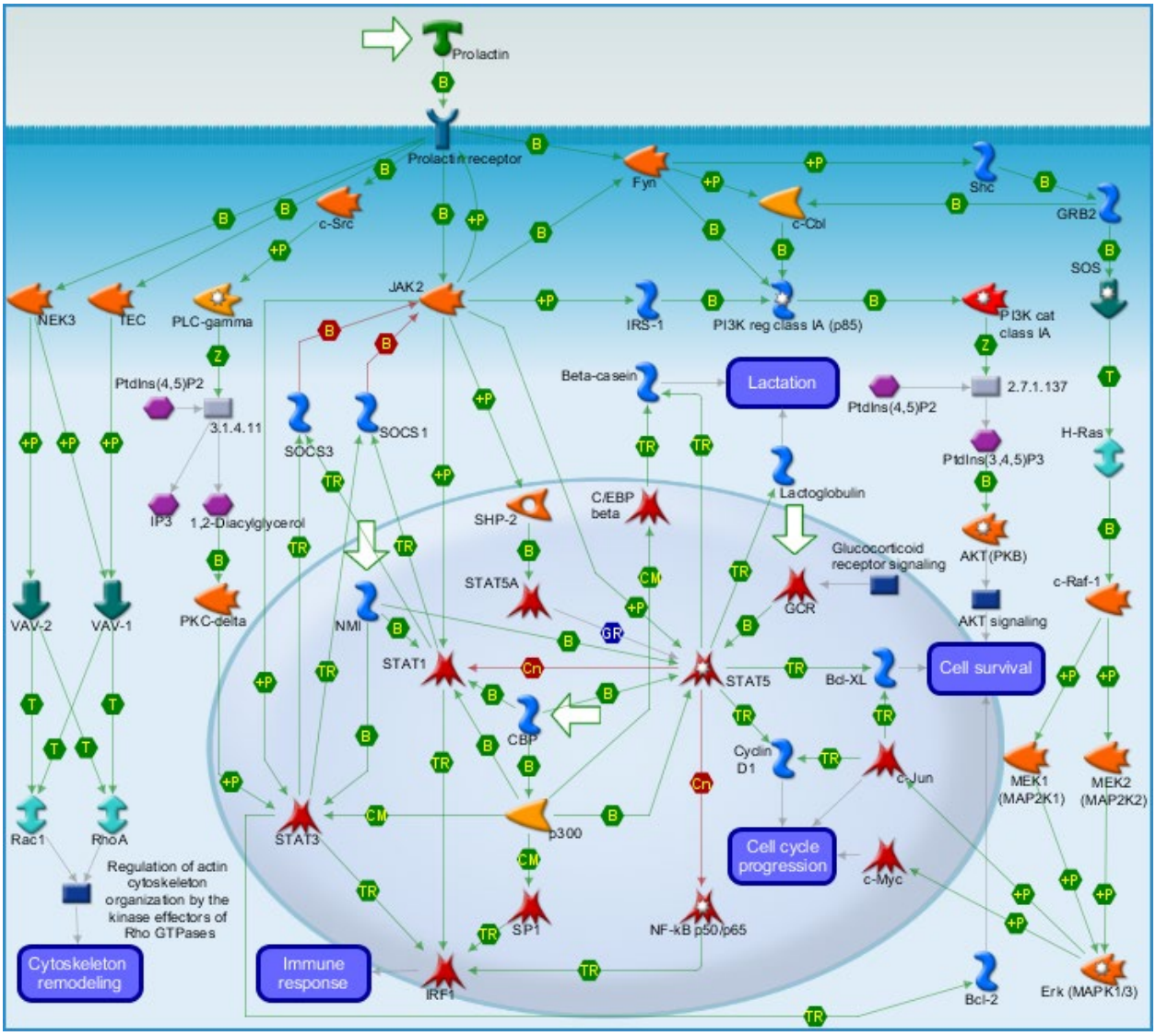

Figure 3. Pathway map showing the interconnected downstream signaling which occurs when prolactin (PRL) binds to prolactin receptor (PRLR). Binding of PRL to the two binding sites of PRLR signals activation of Janus kinase 2 (JAK2) which in turn causes dimerization and phosphorylation of the two PRLR molecules. This conformational change leads to activation and phosphorylation of STAT proteins particularly STAT 1, STAT 3, STAT 5A and STAT 5B. These STAT proteins translocate to the nucleus after dimerization and activate transcription factors required for cell cycle progression, cell survival, immune response, lactation, and cytoskeletal remodeling as described in the figure above. Figure legend can be found using this link (https://portal.genego.com/help/MC_legend.pdf). Map developed using "Metacore by Clarivate" pathway map creator 2.6.0.

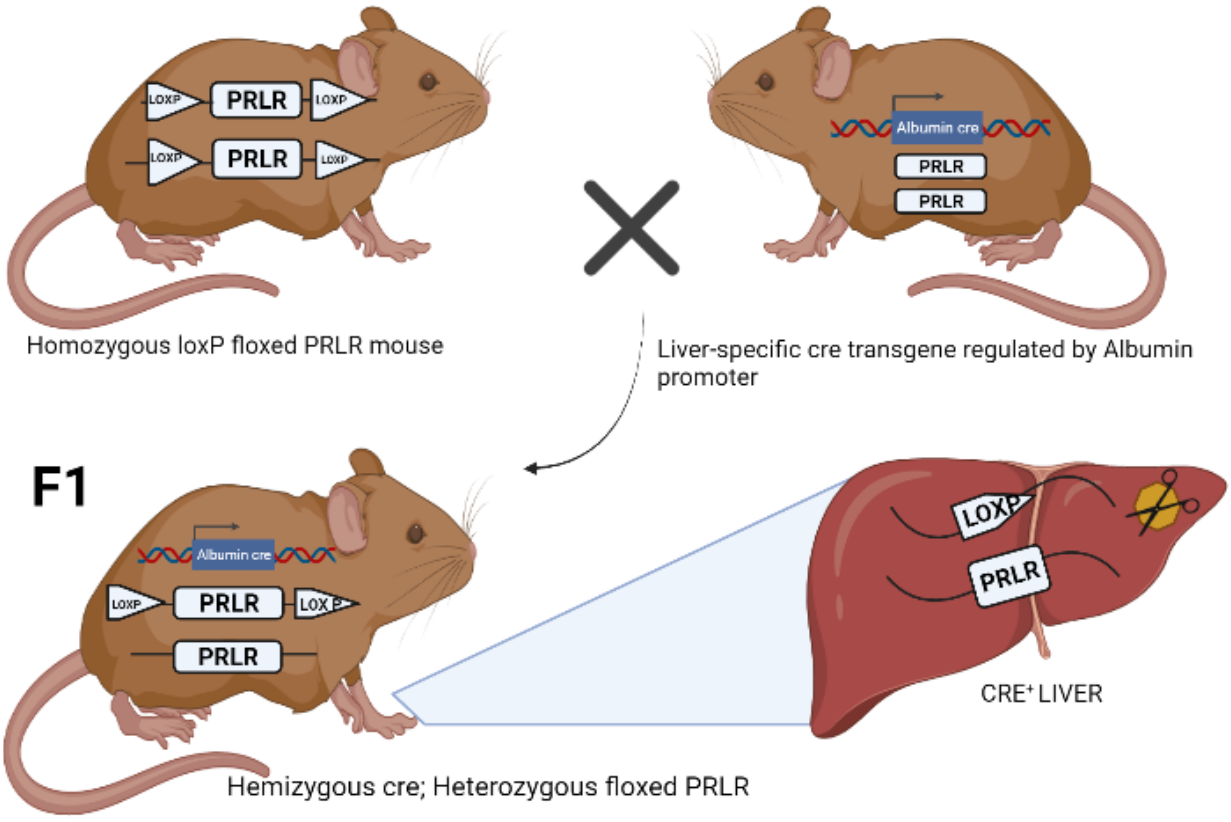

Figure 4. Breeding scheme for generating *Prlr* knockout mice. Homozygous loxP flanked mice were crossed with *Albumin-cre* mice. The F1 generation of these mice were heterozygous for the *Prlr* gene after one breeding. The F1 were then crossed back to the homozygous loxP-flanked mice to generate homozygous *Prlr* knockout mice with a hemizygous cre transgene. Illustration created using Biorender.

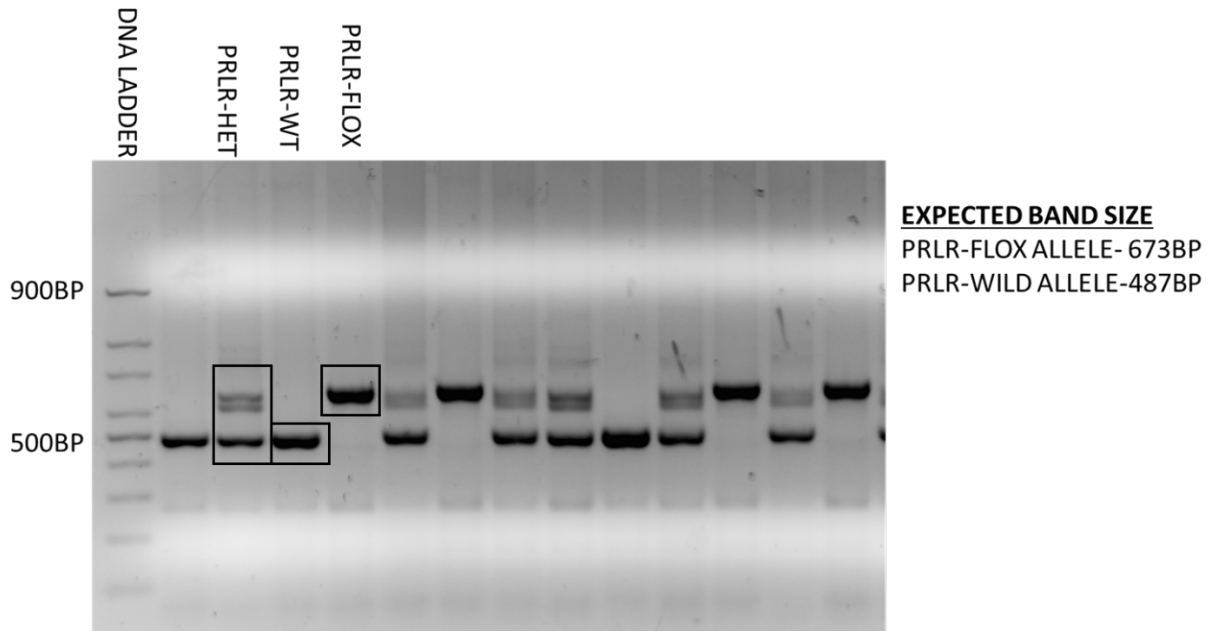

Figure 5. *Prlr* genotyping. Electrophoresis gel image displaying amplified bands of *Prlr* floxed and wild-type alleles.

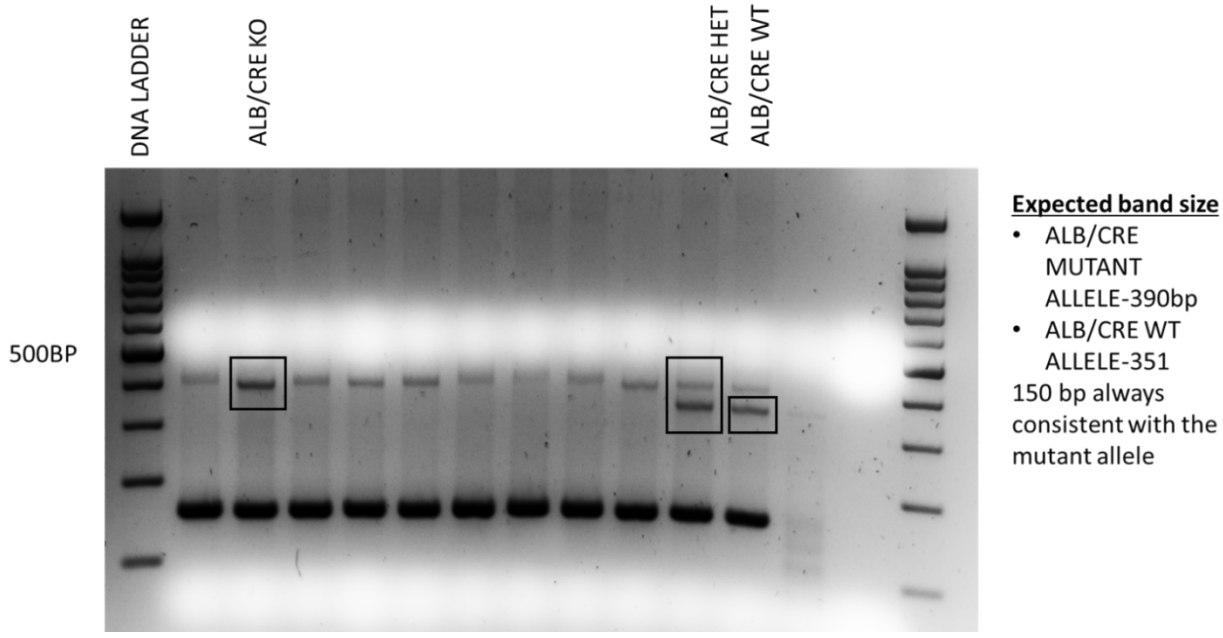

Figure 6. *Albumin-cre* genotyping. Electrophoresis gel image displaying amplified bands of *Albumin-cre* mutant and wild-type alleles.

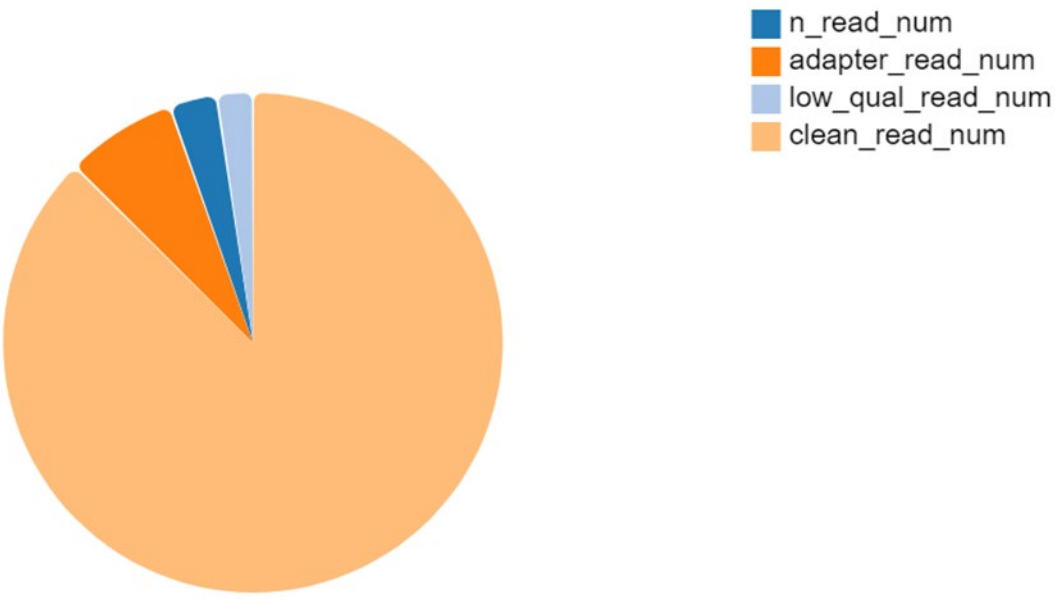

Figure 7. Pie chart showing statistics of filtered reads. N represents the number of reads with an unknown base (less than 5% of the proportion of total raw reads); Adapter: the number of reads containing adapters (contaminated by the adapter); Low Quality: low-quality reads (the proportion of bases with a quality score below 15); Clean Reads: proportion of clean filtered reads to the total raw reads.

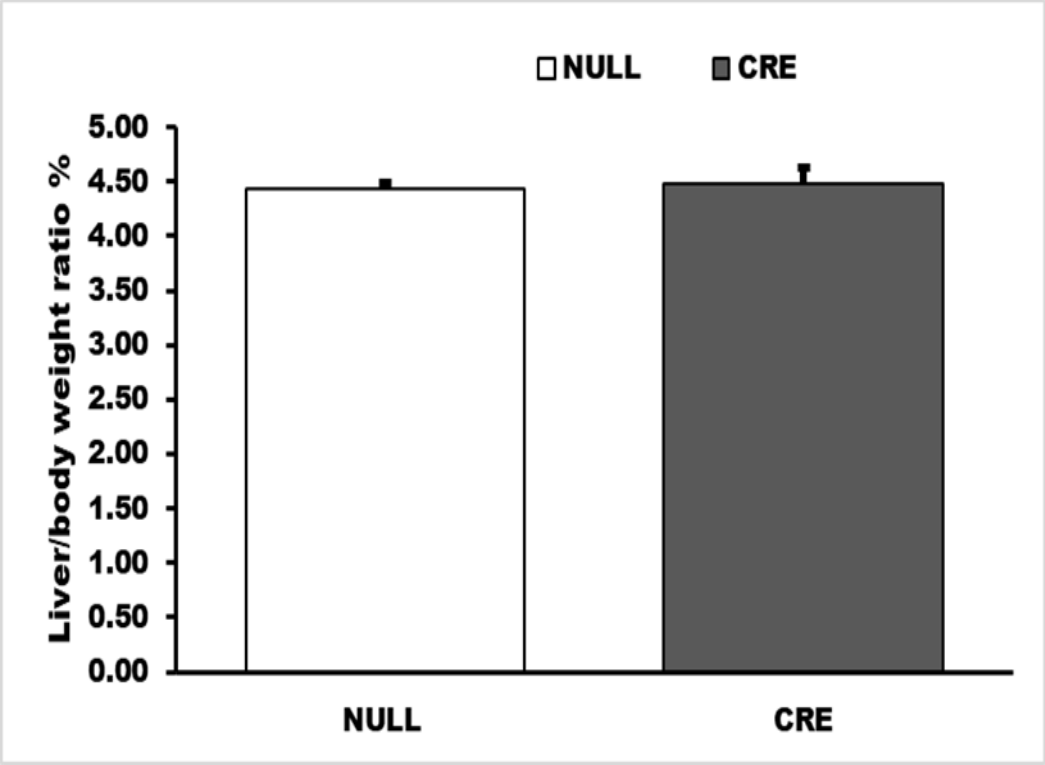

Figure 8. Average percentage of liver-to-body weight ratio compared between null-virus and cre-virus treated mice. The relative liver weight to body weight was calculated as a percentage of their ratio with significance defined when $P<0.05$. Data is expressed as mean ± SEM (n=5).

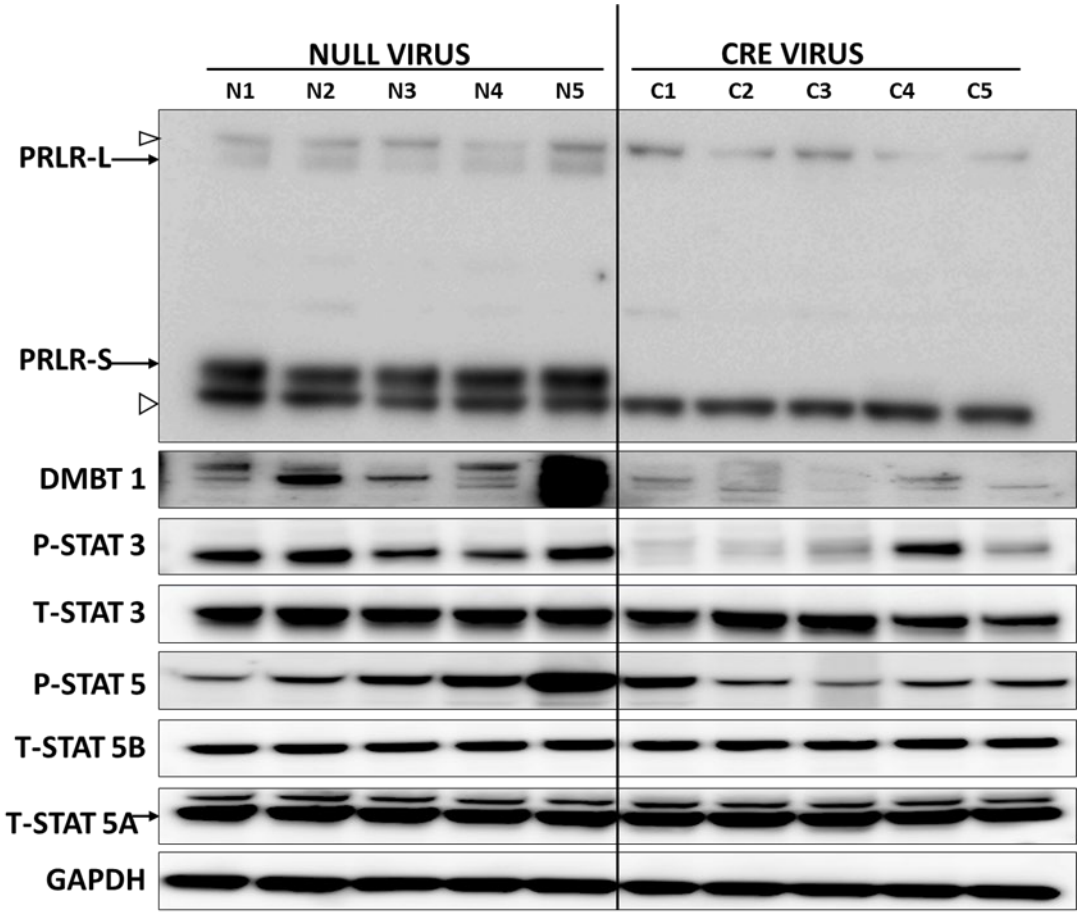

Figure 9. Western blot analysis of protein expression in livers of null or cre virus-treated mice. The apparent molecular weight of each protein is indicated in Table 2. Open triangles refer to non-specific bands. GAPDH serves as the internal loading control. Relative quantification of the level of protein expression by the various biological replicates is shown in Figure 10. (Lanes N1 to N5 represent biological replicates belonging to the null-virus set whilst lanes C1 to C5 represents biological replicates of the cre-virus batch). (PRLR-L: long isoform of prolactin receptor; PRLR-S: short isoform of prolactin receptor; DMBT-1: deleted in malignant brain tumors 1; p-STAT 3: phosphorylated signal transducer and activation of transcription 3; T-STAT3: total STAT3; p-STAT5: phosphorylated STAT5; T-STAT5 A and 5B: total STAT5A and 5B; GAPDH: glyceraldehyde 3-phosphate dehydrogenase).

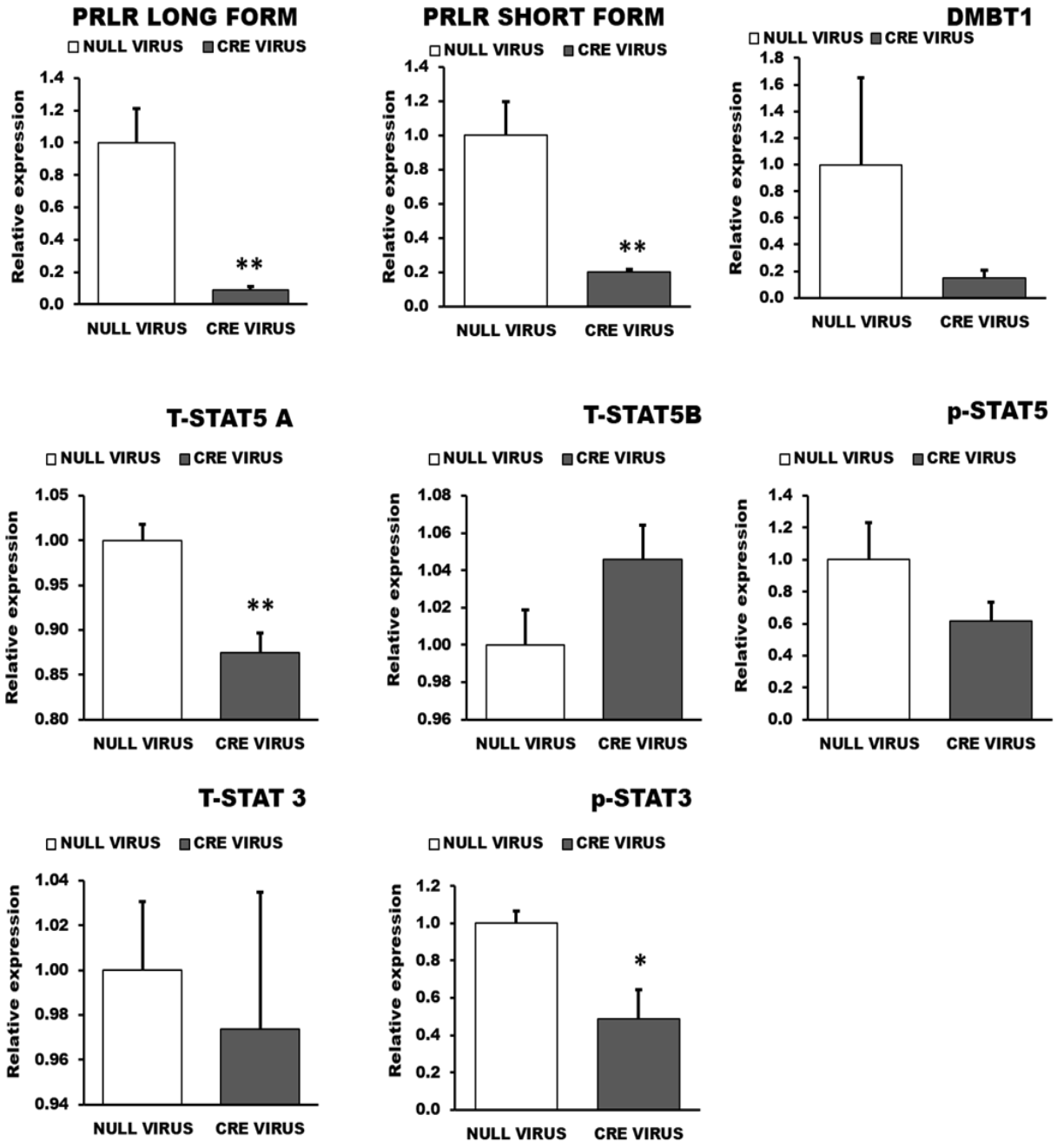

Figure 10. Bar graphs of the relative quantification of protein levels. Densitometric analysis was performed using Image J software. With GAPDH as a housekeeping gene, relative levels of the various proteins were expressed as a ratio of their densitometric values to the densitometric values of the null virus. Error bars indicate significance with * P value ≤ 0.05, **P≤ 0.01, ***P≤ 0.001; n=5.

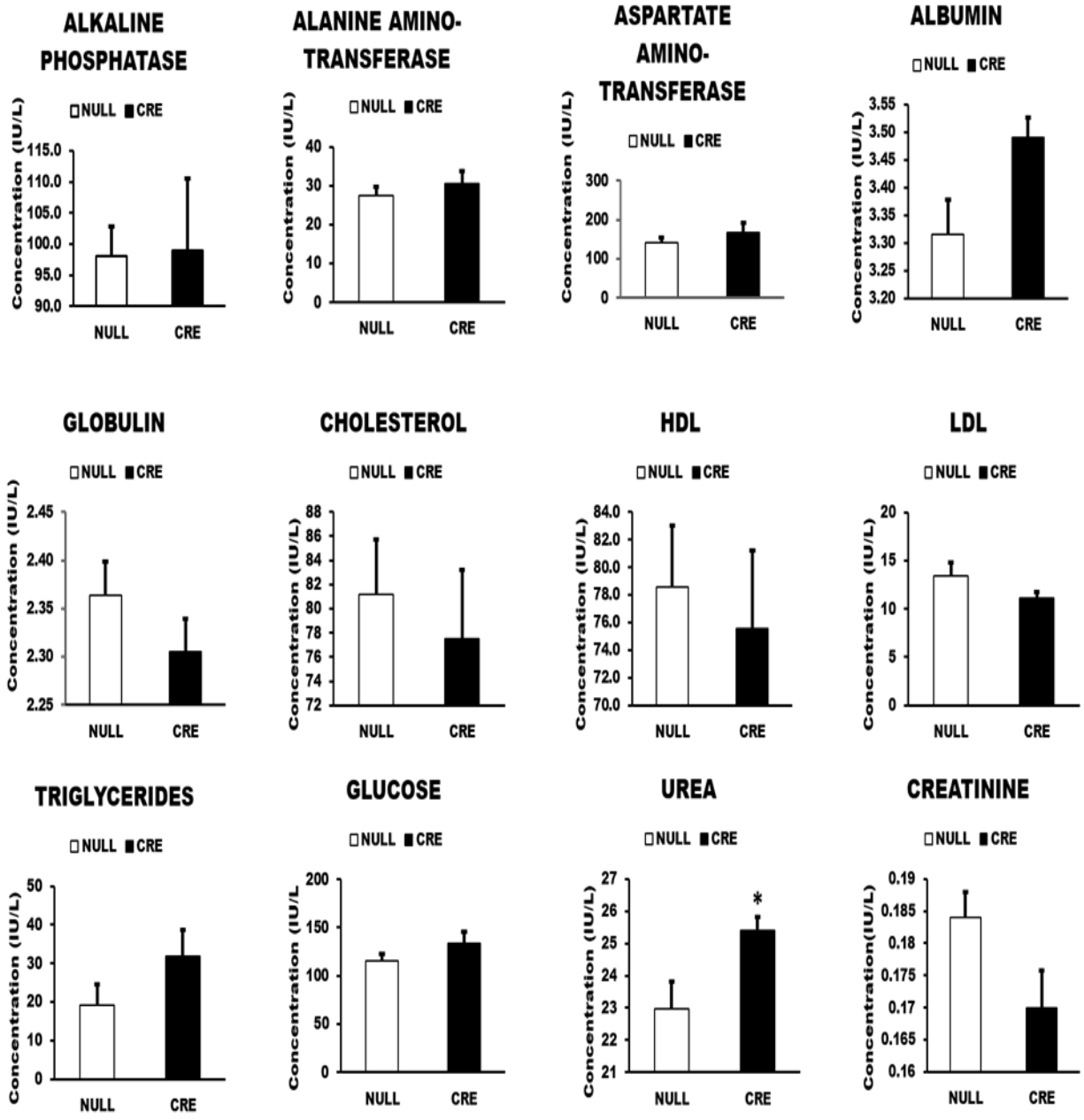

Figure 11.Serum biochemistry of blood samples collected from mice injected with AAV8-null virus and AAV8-cre virus. (HDL- high density lipoproteins; LDL- low density lipoproteins). Error bars indicate significance with * P value ≤ 0.05, **P≤ 0.01, ***P≤ 0.001.

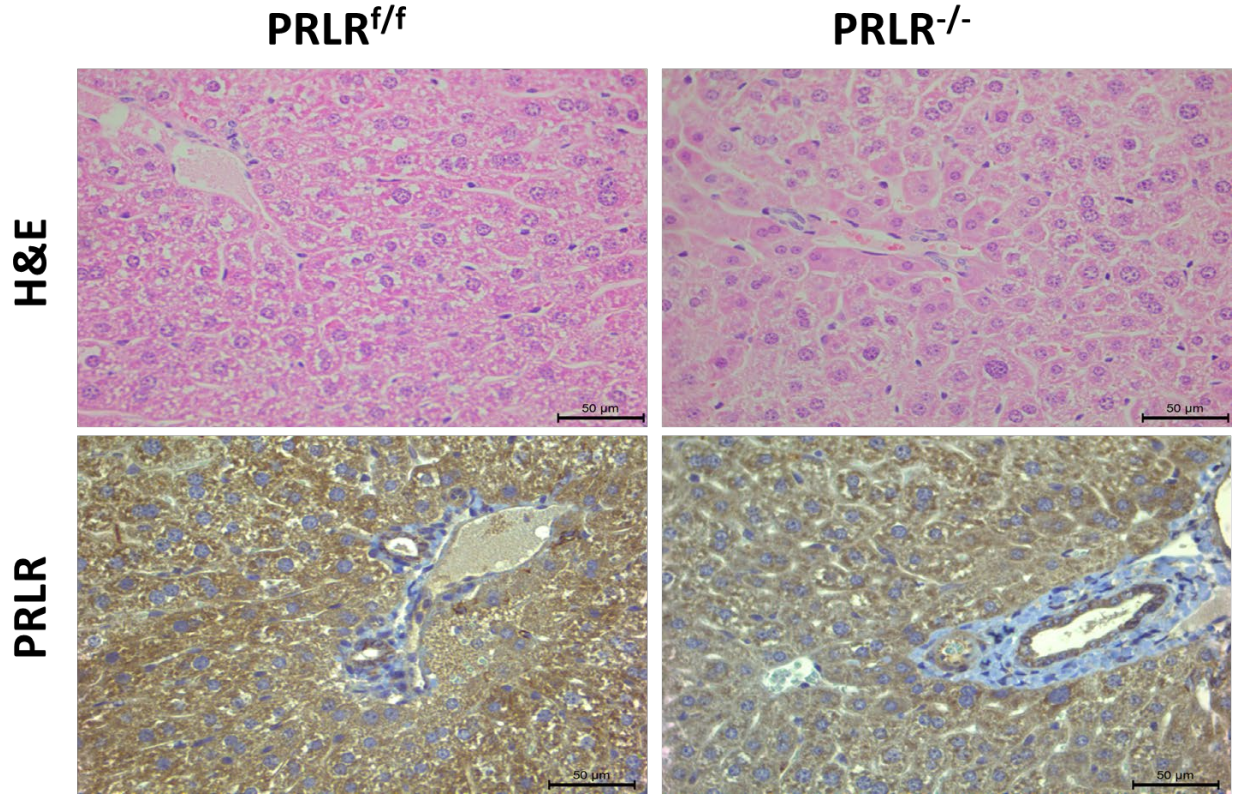

Figure 12.Immunohistochemical analysis of PRLR protein expression in floxed and knockout mouse livers shown by brown deposits in cytosol of hepatocytes and ductal cells. Magnification at 400X.

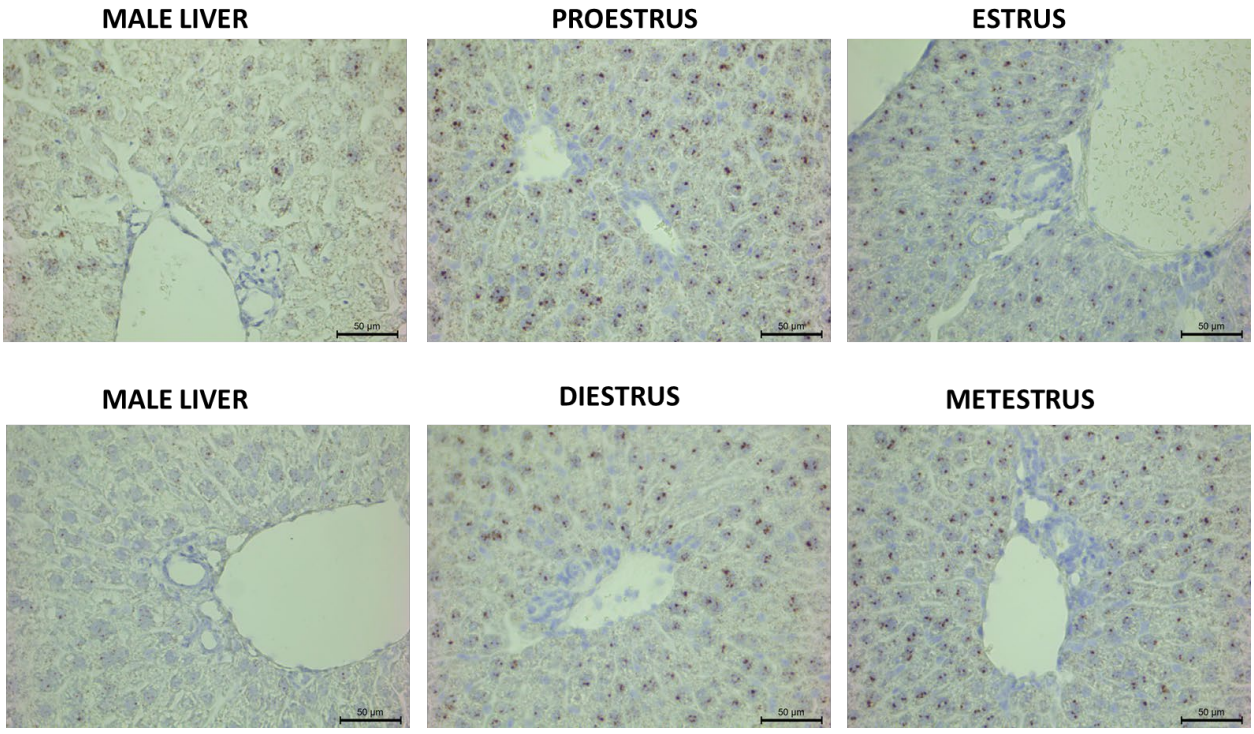

Figure 13. In-situ hybridization of *Prlr* mRNA in male and female mouse livers harvested at the various stages of their estrous cycles. Magnification at 400X.

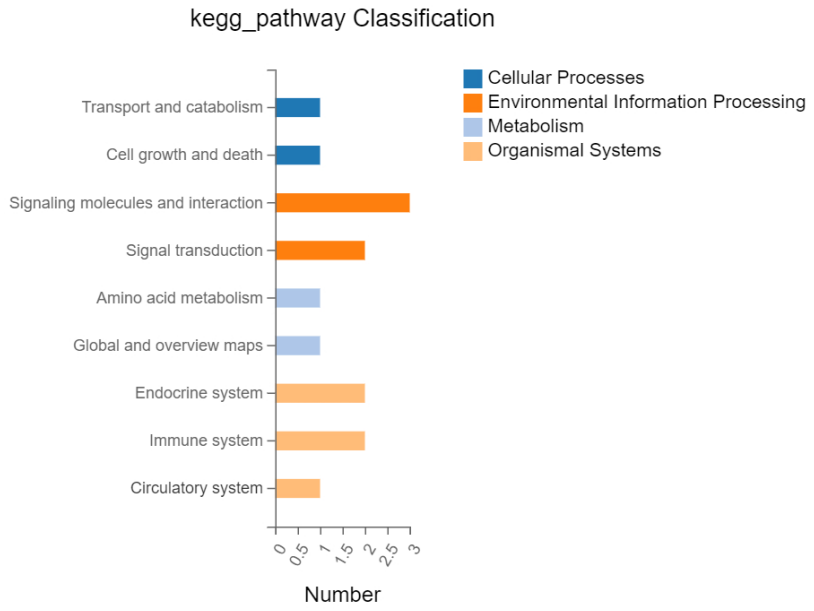

A.

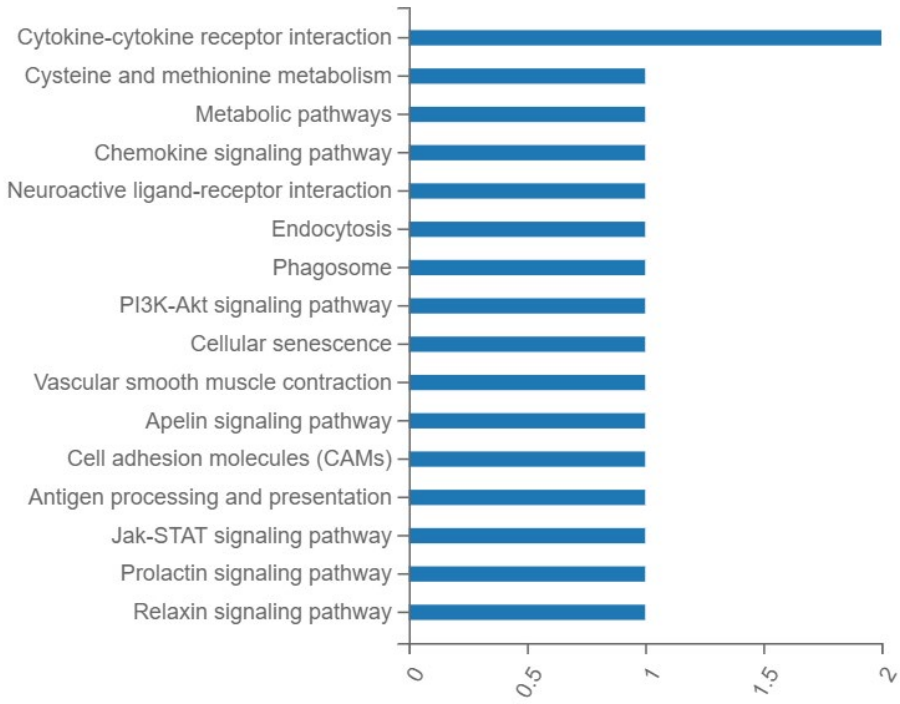

B.

Figure 14. KEGG pathway analysis shown in panels A and B. The x-axes in both images represent the number of genes annotated to a category of KEGG pathway whilst both y-axes represent the category of KEGG pathway.

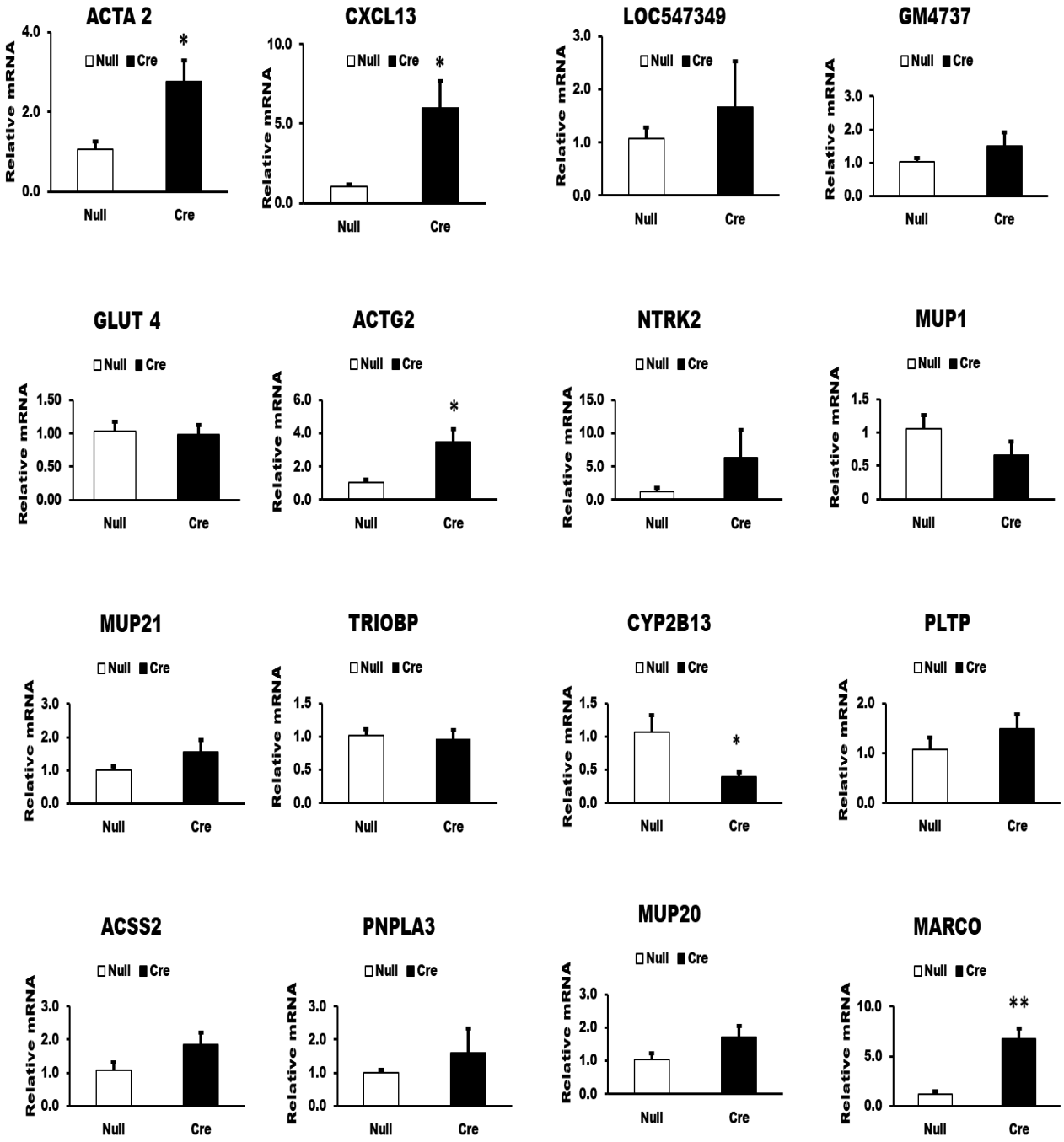

Figure 15. Quantitative real-time polymerase chain reaction analysis of some upregulated and downregulated genes after hepatocyte-specific deletion of *Prlr*. For all bar charts, error bars indicate significance with * P value ≤ 0.05, **P≤ 0.01, ***P≤ 0.001.

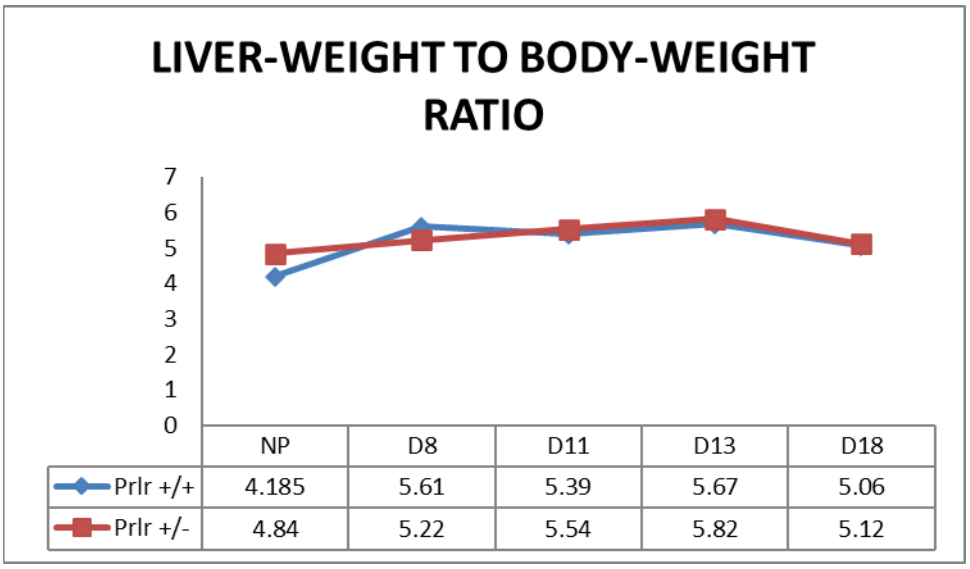

Figure 16. Liver to body-weight ratios of heterozygous and wild-type female mice both in non-pregnant and pregnant states.

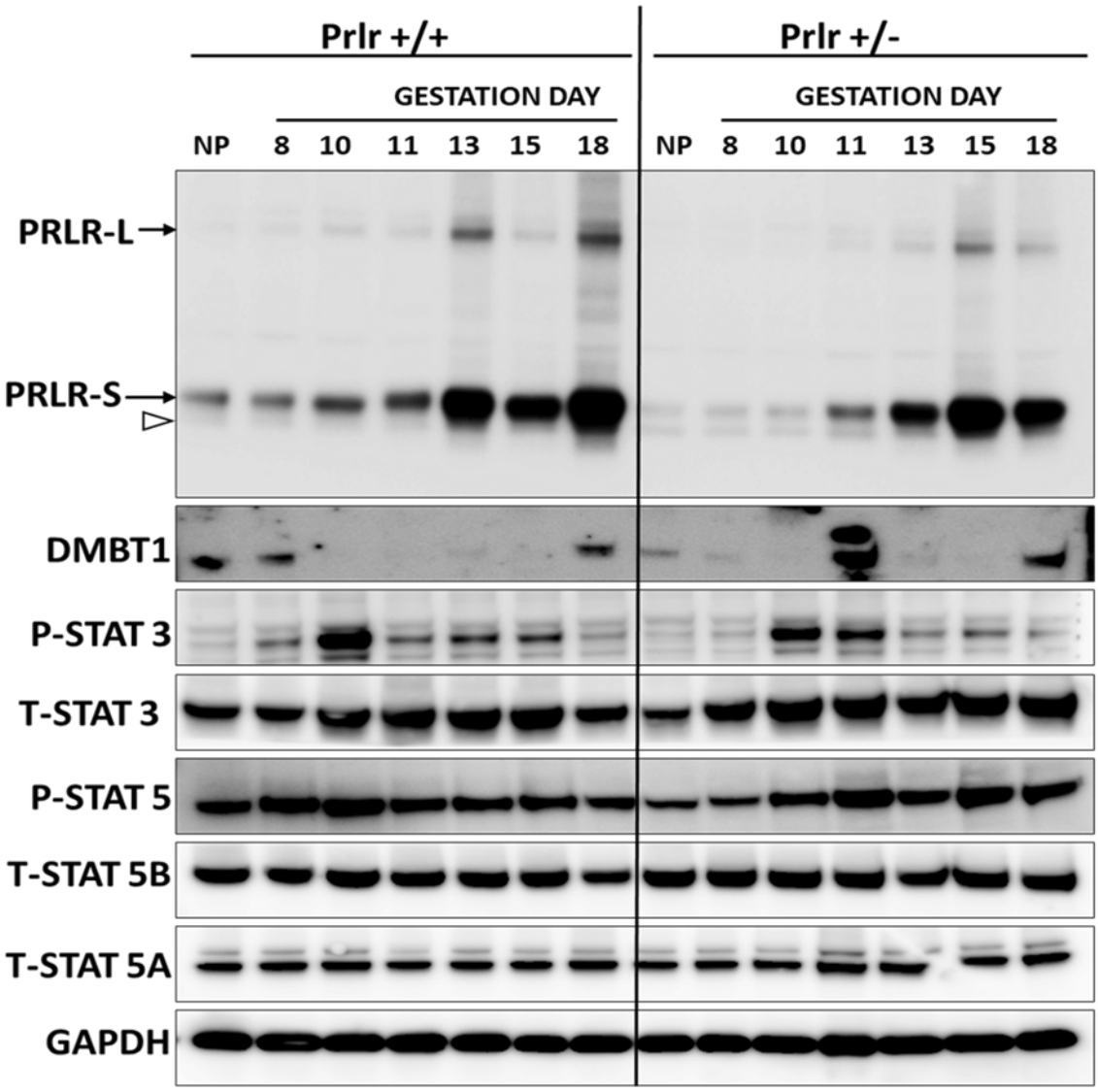

Figure 17. Western blot analysis of protein expression in livers of wild-type and heterozygous non-pregnant and pregnant mice. The apparent molecular weight of each protein is indicated in Table 2. Open triangles refer to non-specific bands. GAPDH serves as the internal loading control. (PRLR-L: long isoform of prolactin receptor; PRLR-S: short isoform of prolactin receptor; DMBT-1: deleted in malignant brain tumors 1; p-STAT 3: phosphorylated signal transducer and activation of transcription 3; T-STAT3: total STAT3; p-STAT5: phosphorylated STAT5; T-STAT5 A and 5B: total STAT5A and 5B; GAPDH: glyceraldehyde 3-phosphate dehydrogenase).

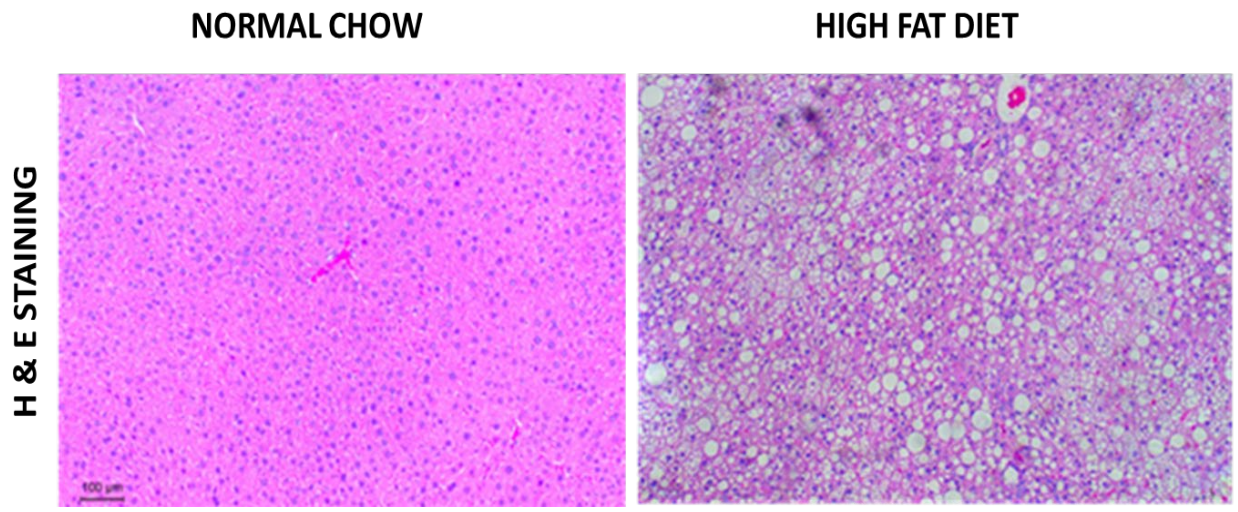

Figure 18. Histological assessment of liver sections from male mice fed with standard chow or high fat diet using hematoxylin and eosin staining. Liver fat seen as white round droplets. Magnification at 100X.

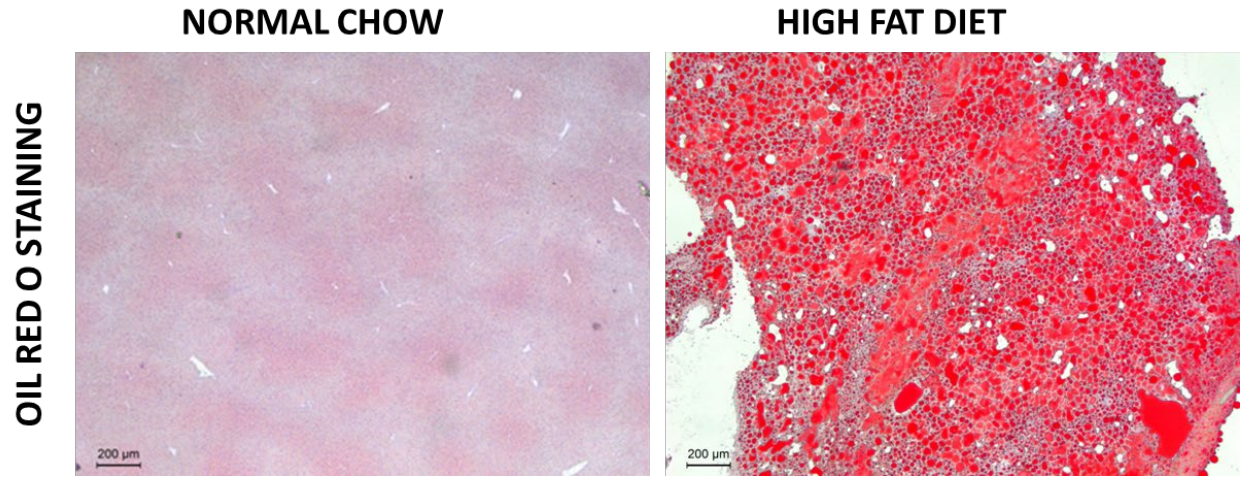

Figure 19. Oil red o staining of livers of mice fed with standard chow and mice fed with high fat to visualize fat deposition and accumulation. Fat deposits stain red.

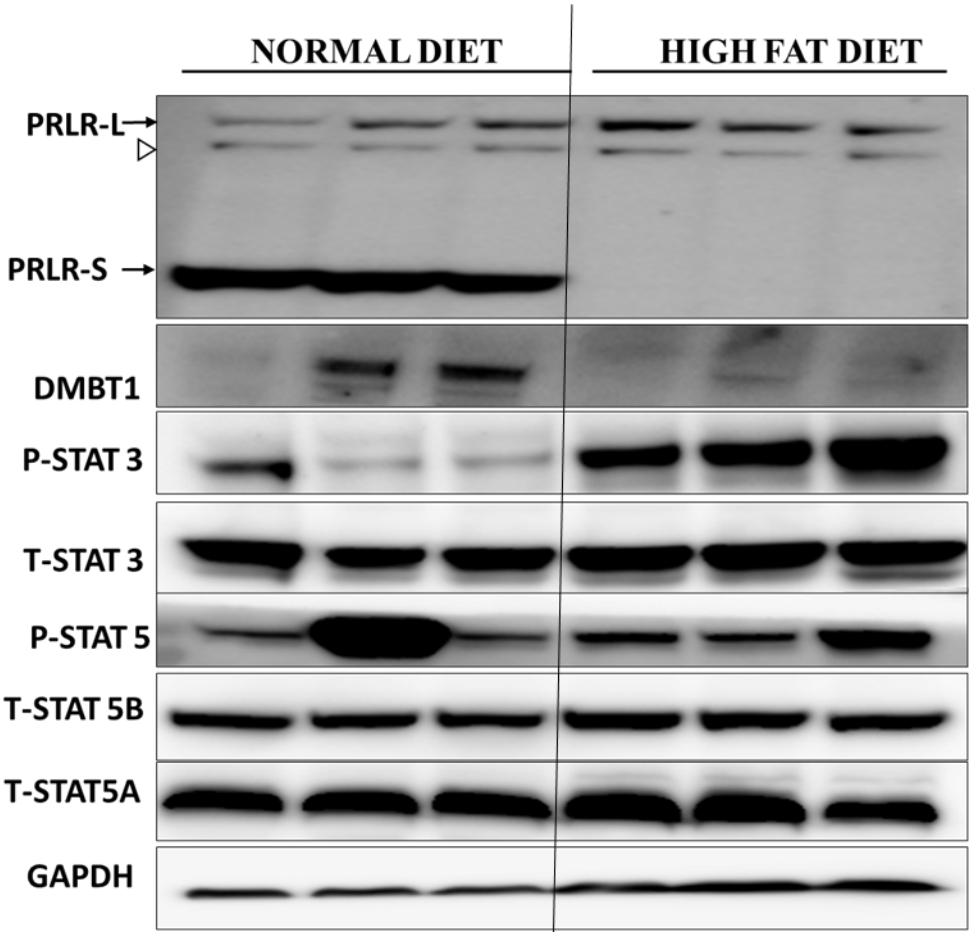

Figure 20. Western blot analysis of protein expression in livers of mice fed with normal chow versus mice fed with high fat diet. The apparent molecular weight of each protein is indicated in Table 2. Open triangles refer to non-specific bands. GAPDH serves as the internal loading control. (PRLR-L: long isoform of prolactin receptor; PRLR-S: short isoform of prolactin receptor; DMBT-1: deleted in malignant brain tumors 1; p-STAT 3: phosphorylated STAT3; T-STAT3: total STAT3; p-STAT5: phosphorylated STAT5; T-STAT5 A and 5B: total STAT 5A and 5B; GAPDH: glyceraldehyde 3-phosphate dehydrogenase). n=3.

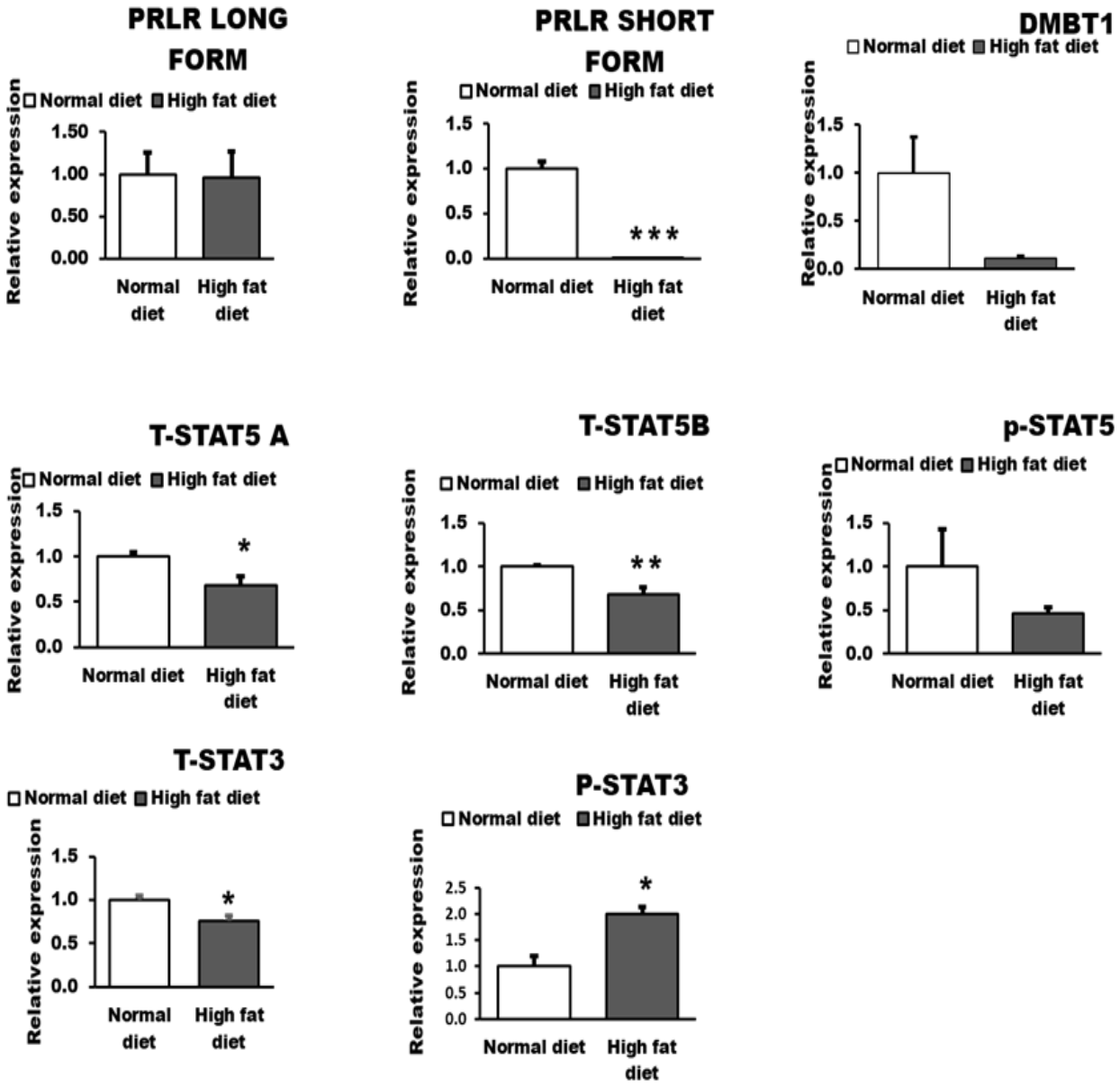

Figure 21. Densitometric analysis of protein bands projected as bar charts. This was performed using Image J software. Relative levels of the various proteins were expressed as a ratio of their densitometric values to the densitometric values of normal diet-fed mouse livers. Error bars indicate significance with * P value ≤ 0.05, **P≤ 0.01, ***P≤ 0.001;n=3.

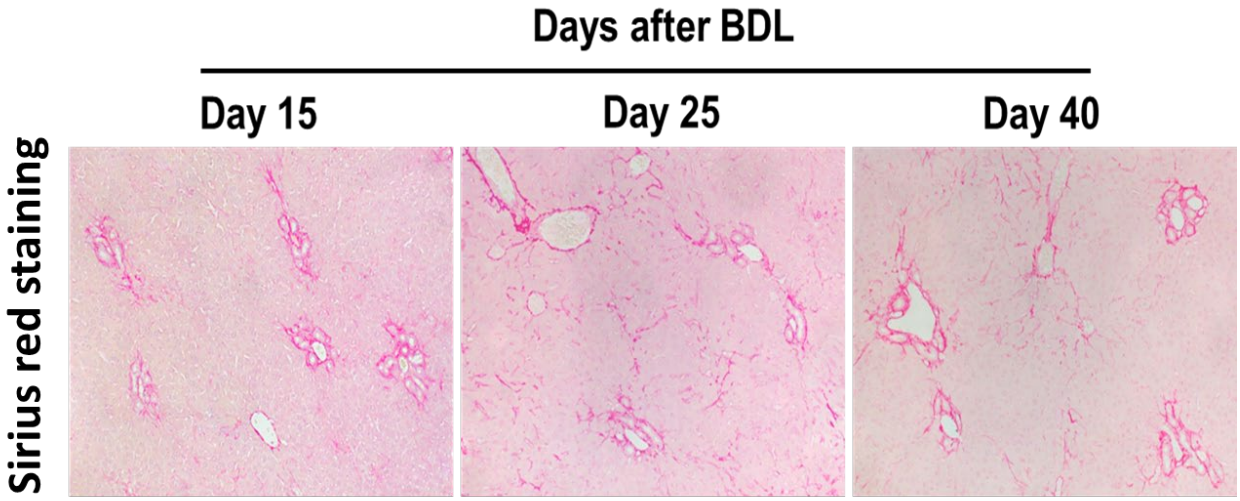

Figure 22. Sirius red staining of livers collected from mice post surgeries at different timepoints to reveal hepatic collagen in fibrotic response to bile duct ligation (BDL). Magnification at 200X.

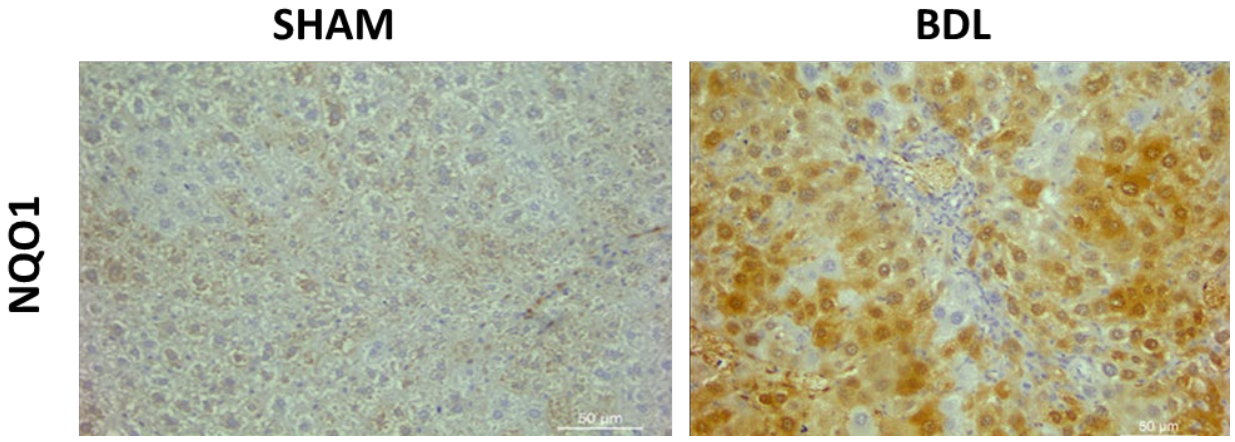

Figure 23. NQO1 immunostaining of livers collected from sham and bile duct ligated (BDL) mice. Magnification at 400X.

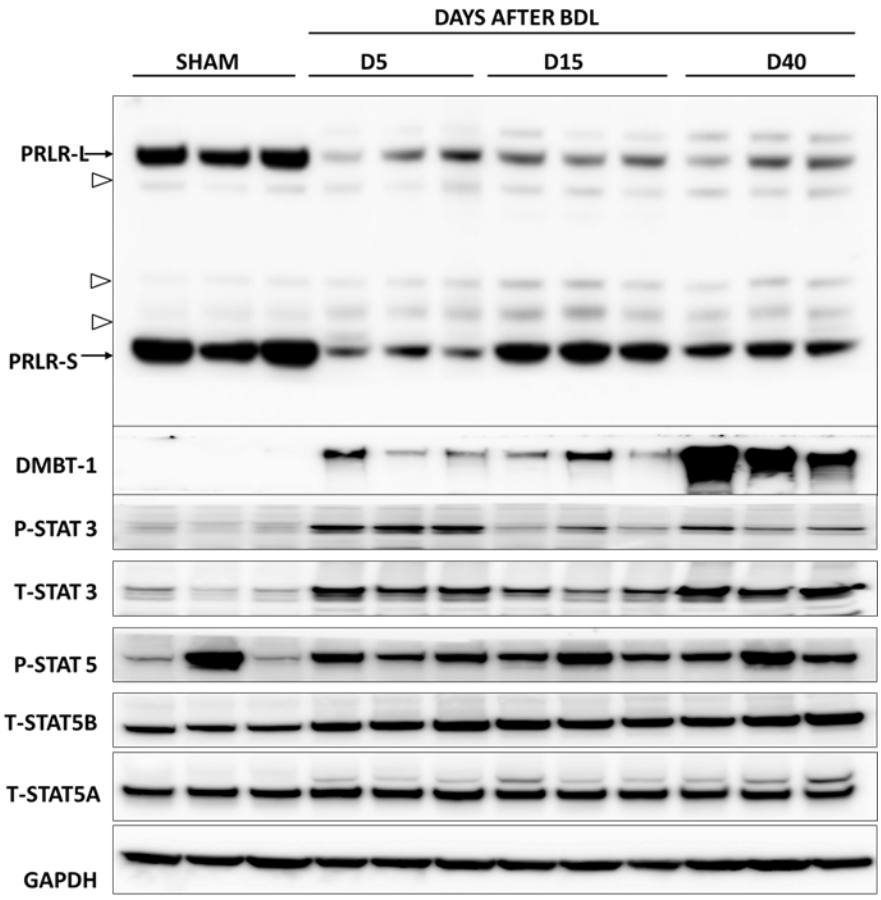

Figure 24. Western blot analysis of protein expression in livers of sham mice and bile duct ligated mice at different timepoints. The apparent molecular weight of each protein is indicated in Table 2. Open triangles refer to non-specific bands. GAPDH serves as the internal loading control. (PRLR-L: long isoform of prolactin receptor; PRLR-S: short isoform of prolactin receptor; DMBT-1: deleted in malignant brain tumors 1; p-STAT 3: phosphorylated signal transducer and activation of transcription 3; T-STAT3: total STAT3; p-STAT5: phosphorylated STAT5; T-STAT5 A and 5B: total STAT 5A and 5B; GAPDH: glyceraldehyde 3-phosphate dehydrogenase). n=3 for each timepoint.

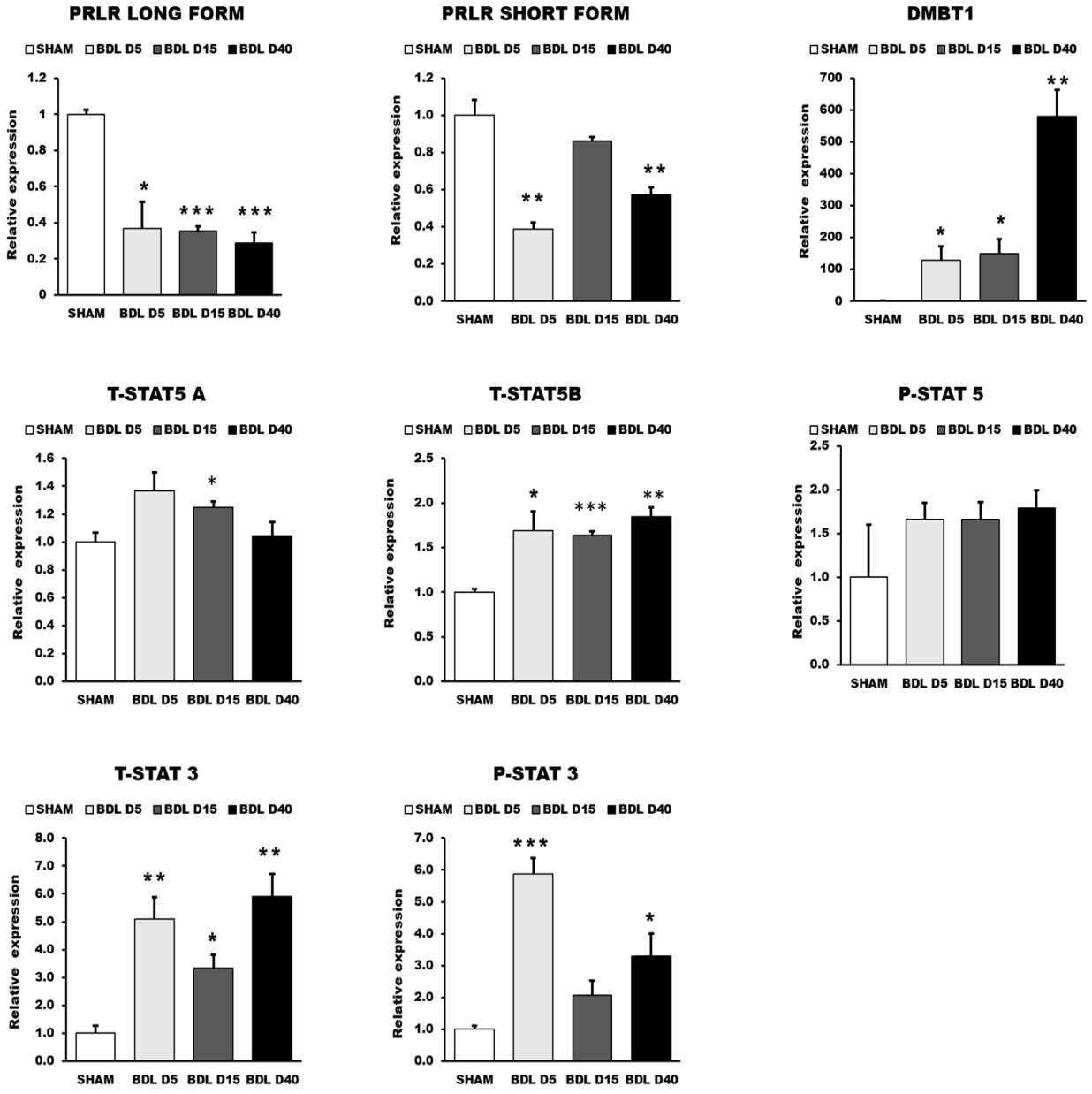

Figure 25. Bar graphs of the quantification of protein levels relative to the sham controls. Densitometric analysis was performed using Image J software. Relative levels of the various proteins were expressed as a ratio of their densitometric values to the densitometric values of sham livers. Error bars indicate significance with * P value ≤ 0.05, **P≤ 0.01, ***P≤ 0.001; n=5.

TABLES

Table 1. List of primers used for genotyping PCR

PRIMER NAME	**PRIMER TYPE**	**SEQUENCE 5'---------> 3'**
Prlr-Flox Forward	Common Forward	ATGCCACTTTCCAAGGTCTG
Prlr-Flox Reverse	Common Reverse	CCCTCCAGTGCTCTGATGTT
Alb-cre (20239)	Wild Type Forward	TGCAAACATCACATGCACAC
Alb-cre (20240)	Common	TTGGCCCCTTACCATAACTG
Alb-cre (OIMR5374)	Mutant Forward	GAAGCAGAAGCTTAGGAAGATGG
Prlr (oIMR1168)	Mutant	GCTTCCTCTTGCAAAACCACACTGC
Prlr (oIMR3089)	Wild-type	CACAGTAAATGCCACGAACG
Prlr (oIMR3090)	Common	CCTCCCTTTCCAGAAAGCAT

Table 2. List of antibodies used in western blot

PROTEIN	MOLECULAR WEIGHT	PRIMARY ANTIBODY	BLOCKING BUFFER	DILUTION	SECONDARY ANTIBODY	DILUTION	EXPOSURE TIME
GAPDH	~37kDa	GAPDH Rabbit mAb (D16H11) XP(R); Cell Signaling	5% Non-fat dry milk	1:3000	Goat anti-rabbit IgG (H+L) HRP conjugate (170-6515;Biorad)	1:10,000	30 secs
T-STAT3	~86kDa	STAT3 Rabbit mAb (79D7); Cell Signaling	5% Bovine serum albumin	1:2000	Goat anti-rabbit IgG (H+L) HRP conjugate (170-6515;Biorad)	1:10,000	2 mins
T-STAT5a	~92kDa	Anti-STAT5a ,Rabbit pAb (100735-T46); HD090C160973; Sino Biological	5% Bovine serum albumin	1:1000	Goat anti-rabbit IgG (H+L) HRP conjugate (170-6515;Biorad)	1:10,000	1min
T-STAT5b	~90kDa	STAT5b Rabbit pAb (34662); Cell Signaling	5% Bovine serum albumin	1:1000	Goat anti-rabbit IgG (H+L) HRP conjugate (170-6515;Biorad)	1:10,000	2 mins
P-STAT 3	~86kDa	p-STAT3 (Y705) D3 A7(XP) (TM) Rabbit mAb; Cell Signaling	5% Bovine serum albumin	1:2000	Goat anti-rabbit IgG (H+L) HRP conjugate (170-6515;Biorad)	1:10,000	1 hour
P-STAT 5	~90kDa	p-STAT5(Tyr694) (D47E7) XP Rabbit mAb (4322) Cell Signaling	5% Bovine serum albumin	1:2000	Goat anti-rabbit IgG (H+L) HRP conjugate (170-6515;Biorad)	1:10,000	1 hour
DMBT1	~235kDa	Anti-DMBT1 Affinity Purified Goat IgG (AF5915) R&D systems	5% Non-fat dry milk	1:300	Bovine anti-goat IgG (H+L) Peroxidase conjugated (805-035-180; Jackson ImmunoResearch)	1:10,000	1 hour
PRLR	Short-~45kDa Long-~95kDa	PRLR Rabbit PAb (50457-T16/HD11SE0515); Sino Biological	5% Non-fat dry milk	1:2000	Goat anti-rabbit IgG (H+L) HRP conjugate (170-6515;Biorad)	1:10,000	1 hour

Table 3. List of primers used for qRT-PCR

GENE	ASSAY ID	CATALOG NO.
18S RNA	Mm03928990_g1	4331182
ACTA 1	Mm00808218_g1	4331182
ACTA 2	Mm01546133_m1	4331182
CXCL13	Mm00444534_m1	4331182
LOC 547349	Mm03033061_u1	4351372
AHCY; GM47349	Mm01742465_SH	4331182
ACTG2	Mm00656102_m1	4453320
SCL2A4/ GLUT4	Mm00436615_m1	4453320
TIMP 1	Mm01341361_m1	4453320
NTRK 2	Mm00435422_m1	4453320
MUP 1	Mm04204590_gH	4448892
MUP 20	Mm02343630_g1	4448892
MUP 21	Mm07306356_m1	4448892
TRIOBP	Mm00661904_m1	444889
CYP2B13	Mm00771172_g1	4331182
PLTP	Mm01240573_m1	4331182
PNPLA3	Mm00504421_m1	4351372
ACSS2	Mm00480101_m1	4331182
ALB	Mm00802090_m1	4331182

REFERENCES

1. Wang, F.S., et al., *The global burden of liver disease: the major impact of China.* Hepatology, 2014. **60**(6): p. 2099-108.
2. Anstee, Q.M., et al., *From NASH to HCC: current concepts and future challenges.* Nat Rev Gastroenterol Hepatol, 2019. **16**(7): p. 411-428.
3. Temple, J.L., et al., *A Guide to Non-Alcoholic Fatty Liver Disease in Childhood and Adolescence.* Int J Mol Sci, 2016. **17**(6).
4. Cobbina, E. and F. Akhlaghi, *Non-alcoholic fatty liver disease (NAFLD) - pathogenesis, classification, and effect on drug metabolizing enzymes and transporters.* Drug Metab Rev, 2017. **49**(2): p. 197-211.
5. Bogdanos, D.P., B. Gao, and M.E. Gershwin, *Liver immunology.* Compr Physiol, 2013. **3**(2): p. 567-98.
6. Juza, R.M. and E.M. Pauli, *Clinical and surgical anatomy of the liver: a review for clinicians.* Clin Anat, 2014. **27**(5): p. 764-9.
7. Liau, K.H., L.H. Blumgart, and R.P. DeMatteo, *Segment-oriented approach to liver resection.* Surgical Clinics of North America, 2004. **84**(2): p. 543-561.
8. Lorente, S., M. Hautefeuille, and A. Sanchez-Cedillo, *The liver, a functionalized vascular structure.* Sci Rep, 2020. **10**(1): p. 16194.
9. Sasse, D., U.M. Spornitz, and I.P. Maly, *Liver architecture.* Enzyme, 1992. **46**(1-3): p. 8-32.
10. Annunziato, S. and J.S. Tchorz, *Liver zonation-a journey through space and time.* Nat Metab, 2021. **3**(1): p. 7-8.
11. Kietzmann, T., *Metabolic zonation of the liver: The oxygen gradient revisited.* Redox Biol, 2017. **11**: p. 622-630.
12. Diamantis, I. and D.T. Boumpas, *Autoimmune hepatitis: evolving concepts.* Autoimmun Rev, 2004. **3**(3): p. 207-14.
13. Ben-Moshe, S. and S. Itzkovitz, *Spatial heterogeneity in the mammalian liver.* Nat Rev Gastroenterol Hepatol, 2019. **16**(7): p. 395-410.
14. Jungermann, K. and N. Katz, *Functional specialization of different hepatocyte populations.* Physiol Rev, 1989. **69**(3): p. 708-64.
15. Schleicher, J., et al., *Zonation of hepatic fatty acid metabolism - The diversity of its regulation and the benefit of modeling.* Biochim Biophys Acta, 2015. **1851**(5): p. 641-56.
16. Fanti, M., et al., *Tri-iodothyronine induces hepatocyte proliferation by protein kinase a-dependent β-catenin activation in rodents.* Hepatology, 2014. **59**(6): p. 2309-2320.
17. Gebhardt, R., *Metabolic zonation of the liver: regulation and implications for liver function.* Pharmacol Ther, 1992. **53**(3): p. 275-354.

18. Jungermann, K. and T. Kietzmann, *Zonation of parenchymal and nonparenchymal metabolism in liver.* Annu Rev Nutr, 1996. **16**: p. 179-203.

19. Ippoliti, R., et al., *Endocytosis of a chimera between human pro-urokinase and the plant toxin saporin: an unusual internalization mechanism.* Faseb j, 2000. **14**(10): p. 1335-44.

20. Godoy, P., et al., *Recent advances in 2D and 3D in vitro systems using primary hepatocytes, alternative hepatocyte sources and non-parenchymal liver cells and their use in investigating mechanisms of hepatotoxicity, cell signaling and ADME.* Arch Toxicol, 2013. **87**(8): p. 1315-530.

21. Lauschke, V.M., et al., *3D Primary Hepatocyte Culture Systems for Analyses of Liver Diseases, Drug Metabolism, and Toxicity: Emerging Culture Paradigms and Applications.* Biotechnol J, 2019. **14**(7): p. e1800347.

22. Grant, D.M., *Detoxification pathways in the liver.* J Inherit Metab Dis, 1991. **14**(4): p. 421-30.

23. Zamora-Valdes, D. and J.K. Heimbach, *Liver Transplant for Cholangiocarcinoma.* Gastroenterol Clin North Am, 2018. **47**(2): p. 267-280.

24. Tabibian, J.H., et al., *Physiology of cholangiocytes.* Compr Physiol, 2013. **3**(1): p. 541-65.

25. Seki, E. and R.F. Schwabe, *Hepatic inflammation and fibrosis: functional links and key pathways.* Hepatology, 2015. **61**(3): p. 1066-79.

26. Petersen, B.E., et al., *Hepatic oval cells express the hematopoietic stem cell marker Thy-1 in the rat.* Hepatology, 1998. **27**(2): p. 433-45.

27. Fausto, N. and J.S. Campbell, *The role of hepatocytes and oval cells in liver regeneration and repopulation.* Mech Dev, 2003. **120**(1): p. 117-30.

28. Shetty, S., P.F. Lalor, and D.H. Adams, *Liver sinusoidal endothelial cells — gatekeepers of hepatic immunity.* Nature Reviews Gastroenterology & Hepatology, 2018. **15**(9): p. 555-567.

29. Collins, C., et al., *RAG1, RAG2 and pre-T cell receptor alpha chain expression by adult human hepatic T cells: evidence for extrathymic T cell maturation.* Eur J Immunol, 1996. **26**(12): p. 3114-8.

30. Klugewitz, K., et al., *The composition of intrahepatic lymphocytes: shaped by selective recruitment?* Trends Immunol, 2004. **25**(11): p. 590-4.

31. Uyama, N., A. Geerts, and H. Reynaert, *Neural connections between the hypothalamus and the liver.* Anat Rec A Discov Mol Cell Evol Biol, 2004. **280**(1): p. 808-20.

32. Lautt, W.W., *A new paradigm for diabetes and obesity: the hepatic insulin sensitizing substance (HISS) hypothesis.* J Pharmacol Sci, 2004. **95**(1): p. 9-17.

33. Rasouli, M., M. Mosavi-Mehr, and H. Tahmouri, *Liver denervation increases the levels of serum triglyceride and cholesterol via increases in the rate of VLDL secretion.* Clin Res Hepatol Gastroenterol, 2012. **36**(1): p. 60-5.

34. Kiba, T., *The role of the autonomic nervous system in liver regeneration and apoptosis--recent developments.* Digestion, 2002. **66**(2): p. 79-88.

35. Kandilis, A.N., et al., *Liver innervation and hepatic function: new insights.* J Surg Res, 2015. **194**(2): p. 511-519.

36. Masuda, A., et al., *Promotion of liver regeneration and anti-fibrotic effects of the TGF-β receptor kinase inhibitor galunisertib in CCl4-treated mice.* Int J Mol Med, 2020. **46**(1): p. 427-438.

37. Yagi, S., et al., *Liver Regeneration after Hepatectomy and Partial Liver Transplantation.* Int J Mol Sci, 2020. **21**(21).

38. Higgins, G.M., *Experimental pathology of the liver. I. Restoration of the liver of the white rat following partial surgical removal.* Arch Pathol, 1931. **12**: p. 186-202.

39. Mitchell, C. and H. Willenbring, *A reproducible and well-tolerated method for 2/3 partial hepatectomy in mice.* Nat Protoc, 2008. **3**(7): p. 1167-70.

40. Iakova, P., S.S. Awad, and N.A. Timchenko, *Aging reduces proliferative capacities of liver by switching pathways of C/EBPalpha growth arrest.* Cell, 2003. **113**(4): p. 495-506.

41. Desbois-Mouthon, C., et al., *Hepatocyte proliferation during liver regeneration is impaired in mice with liver-specific IGF-1R knockout.* Faseb j, 2006. **20**(6): p. 773-5.

42. Heijboer, A.C., et al., *Sixteen hours of fasting differentially affects hepatic and muscle insulin sensitivity in mice.* J Lipid Res, 2005. **46**(3): p. 582-8.

43. Sinha, A., et al., *Isoflurane hepatotoxicity: a case report and review of the literature.* Am J Gastroenterol, 1996. **91**(11): p. 2406-9.

44. Safari, S., et al., *Hepatotoxicity of halogenated inhalational anesthetics.* Iran Red Crescent Med J, 2014. **16**(9): p. e20153.

45. Liu, W.H., et al., *The Involving Roles of Intrahepatic and Extrahepatic Stem/Progenitor Cells (SPCs) to Liver Regeneration.* Int J Biol Sci, 2016. **12**(8): p. 954-63.

46. Starlinger, P., J.P. Luyendyk, and D.J. Groeneveld, *Hemostasis and Liver Regeneration.* Semin Thromb Hemost, 2020. **46**(6): p. 735-742.

47. Sato, Y., K. Tsukada, and K. Hatakeyama, *Role of shear stress and immune responses in liver regeneration after a partial hepatectomy.* Surg Today, 1999. **29**(1): p. 1-9.

48. Wang, L., et al., *Hepatic vascular endothelial growth factor regulates recruitment of rat liver sinusoidal endothelial cell progenitor cells.* Gastroenterology, 2012. **143**(6): p. 1555-1563.e2.

49. Wang, L., et al., *Liver sinusoidal endothelial cell progenitor cells promote liver regeneration in rats.* J Clin Invest, 2012. **122**(4): p. 1567-73.

50. Poisson, J., et al., *Liver sinusoidal endothelial cells: Physiology and role in liver diseases.* J Hepatol, 2017. **66**(1): p. 212-227.

51. Lee, J., et al., *Pregnancy facilitates maternal liver regeneration after partial hepatectomy.* Am J Physiol Gastrointest Liver Physiol, 2020. **318**(4): p. G772-g780.

52. Arden, K.C., et al., *The receptors for prolactin and growth hormone are localized in the same region of human chromosome 5.* Cytogenet Cell Genet, 1990. **53**(2-3): p. 161-5.

53. Davis, J.A. and D.I. Linzer, *Expression of multiple forms of the prolactin receptor in mouse liver.* Mol Endocrinol, 1989. **3**(4): p. 674-80.

54. Ouhtit, A., G. Morel, and P.A. Kelly, *Visualization of gene expression of short and long forms of prolactin receptor in rat reproductive tissues.* Biol Reprod, 1993. **49**(3): p. 528-36.

55. Abramicheva, P.A. and O.V. Smirnova, *Prolactin Receptor Isoforms as the Basis of Tissue-Specific Action of Prolactin in the Norm and Pathology.* Biochemistry (Mosc), 2019. **84**(4): p. 329-345.

56. Bole-Feysot, C., et al., *Prolactin (PRL) and Its Receptor: Actions, Signal Transduction Pathways and Phenotypes Observed in PRL Receptor Knockout Mice.* Endocrine Reviews, 1998. **19**(3): p. 225-268.

57. Gaytán, F., et al., *Luteolytic effect of prolactin is dependent on the degree of differentiation of luteal cells in the rat.* Biol Reprod, 2001. **65**(2): p. 433-41.

58. Raut, S., S. Deshpande, and N.H. Balasinor, *Unveiling the Role of Prolactin and its Receptor in Male Reproduction.* Horm Metab Res, 2019. **51**(4): p. 215-219.

59. Rubin, R.T., et al., *Secretion of hormones influencing water and electrolyte balance (antidiuretic hormone, aldosterone, prolactin) during sleep in normal adult men.* Psychosom Med, 1978. **40**(1): p. 44-59.

60. Breves, J.P., et al., *Prolactin regulates transcription of the ion uptake Na+/Cl- cotransporter (ncc) gene in zebrafish gill.* Mol Cell Endocrinol, 2013. **369**(1-2): p. 98-106.

61. Ladyman, S.R., et al., *Prolactin receptors in Rip-cre cells, but not in AgRP neurones, are involved in energy homeostasis.* J Neuroendocrinol, 2017. **29**(10).

62. Borba, V.V., G. Zandman-Goddard, and Y. Shoenfeld, *Prolactin and Autoimmunity.* Front Immunol, 2018. **9**: p. 73.

63. Norstedt, G., *A comparison between the effects of growth hormone on prolactin receptors and estrogen receptors in rat liver.* Endocrinology, 1982. **110**(6): p. 2107-12.

64. Esquifino, A.I., M.A. Villanúa, and C. Agrasal, *Possible role of prolactin in growth regulation.* Rev Esp Fisiol, 1987. **43**(4): p. 455-61.

65. Vergani, G., A. Mayerhofer, and A. Bartke, *Acute effects of rat growth hormone (GH), human GH and prolactin on proliferating rat liver cells in vitro: a study of mitotic behaviour and ultrastructural alterations.* Tissue Cell, 1994. **26**(3): p. 457-65.

66. Crowe, P.D., et al., *Prolactin activates protein kinase C and stimulates growth-related gene expression in rat liver.* Mol Cell Endocrinol, 1991. **79**(1-3): p. 29-35.

67. Buckley, A.R., *Prolactin, a lymphocyte growth and survival factor.* Lupus, 2001. **10**(10): p. 684-90.

68. Murphy, P.R., G.E. DiMattia, and H.G. Friesen, *Role of calcium in prolactin-stimulated c-myc gene expression and mitogenesis in Nb2 lymphoma cells.* Endocrinology, 1988. **122**(6): p. 2476-85.

69. Zhou, Y., et al., *A novel bispecific antibody targeting CD3 and prolactin receptor (PRLR) against PRLR-expression breast cancer.* J Exp Clin Cancer Res, 2020. **39**(1): p. 87.

70. Goffin, V., *Prolactin receptor targeting in breast and prostate cancers: New insights into an old challenge.* Pharmacol Ther, 2017. **179**: p. 111-126.

71. Clevenger, C.V., et al., *The role of prolactin in mammary carcinoma.* Endocr Rev, 2003. **24**(1): p. 1-27.

72. Shemanko, C.S., *Prolactin receptor in breast cancer: marker for metastatic risk.* J Mol Endocrinol, 2016. **57**(4): p. R153-r165.

73. Hartwell, H.J., et al., *Prolactin prevents hepatocellular carcinoma by restricting innate immune activation of c-Myc in mice.* Proc Natl Acad Sci U S A, 2014. **111**(31): p. 11455-60.

74. Goffin, V., et al., *Prolactin regulation of the prostate gland: a female player in a male game.* Nat Rev Urol, 2011. **8**(11): p. 597-607.

75. Bartke, A., *Role of growth hormone and prolactin in the control of reproduction: what are we learning from transgenic and knock-out animals?* Steroids, 1999. **64**(9): p. 598-604.

76. Dai, G., et al., *Maternal hepatic growth response to pregnancy in the mouse.* Exp Biol Med (Maywood), 2011. **236**(11): p. 1322-32.

77. Zou, Y., et al., *Nrf2 participates in regulating maternal hepatic adaptations to pregnancy.* J Cell Sci, 2013. **126**(Pt 7): p. 1618-25.

78. Nteeba, J., et al., *Pancreatic prolactin receptor signaling regulates maternal glucose homeostasis.* J Endocrinol, 2019.

79. Huang, C., F. Snider, and J.C. Cross, *Prolactin receptor is required for normal glucose homeostasis and modulation of beta-cell mass during pregnancy.* Endocrinology, 2009. **150**(4): p. 1618-26.

80. Shao, S., et al., *Ablation of prolactin receptor increases hepatic triglyceride accumulation.* Biochem Biophys Res Commun, 2018. **498**(3): p. 693-699.

81. Ponce, A.J., et al., *Low prolactin levels are associated with visceral adipocyte hypertrophy and insulin resistance in humans.* Endocrine, 2020. **67**(2): p. 331-343.

82. Ruiz-Herrera, X., et al., *Prolactin Promotes Adipose Tissue Fitness and Insulin Sensitivity in Obese Males.* Endocrinology, 2017. **158**(1): p. 56-68.

83. Salais-López, H., et al., *Maternal Motivation: Exploring the Roles of Prolactin and Pup Stimuli.* Neuroendocrinology, 2020.

84. Bridges, R.S. and P.M. Ronsheim, *Prolactin (PRL) regulation of maternal behavior in rats: bromocriptine treatment delays and PRL promotes the rapid onset of behavior.* Endocrinology, 1990. **126**(2): p. 837-48.

85. Tian, R.H., et al., *Reducing PRLR expression and JAK2 activity results in an increase in BDNF expression and inhibits the apoptosis of CA3 hippocampal neurons in a chronic mild stress model of depression.* Brain Res, 2019. **1725**: p. 146472.

86. Marano, R.J. and N. Ben-Jonathan, *Minireview: Extrapituitary prolactin: an update on the distribution, regulation, and functions.* Mol Endocrinol, 2014. **28**(5): p. 622-33.

87. Nagy, E. and I. Berczi, *Hypophysectomized rats depend on residual prolactin for survival.* Endocrinology, 1991. **128**(6): p. 2776-84.

88. Torner, L., et al., *In vivo release and gene upregulation of brain prolactin in response to physiological stimuli.* Eur J Neurosci, 2004. **19**(6): p. 1601-8.

89. Tabata, H., et al., *Characterization of multiple first exons in murine prolactin receptor gene and the effect of prolactin on their expression in the choroid plexus.* J Mol Endocrinol, 2012. **48**(2): p. 169-76.

90. Aksamitiene, E., et al., *Prolactin-stimulated activation of ERK1/2 mitogen-activated protein kinases is controlled by PI3-kinase/Rac/PAK signaling pathway in breast cancer cells.* Cell Signal, 2011. **23**(11): p. 1794-805.

91. Elkins, P.A., et al., *Ternary complex between placental lactogen and the extracellular domain of the prolactin receptor.* Nat Struct Biol, 2000. **7**(9): p. 808-15.

92. Freeman, M.E., *A direct effect of the uterus on the surges of prolactin induced by cervical stimulation in the rat.* Endocrinology, 1979. **105**(2): p. 387-90.

93. Kelly, P.A., et al., *Implications of multiple phenotypes observed in prolactin receptor knockout mice.* Front Neuroendocrinol, 2001. **22**(2): p. 140-5.

94. Binart, N., et al., *Rescue of preimplantatory egg development and embryo implantation in prolactin receptor-deficient mice after progesterone administration.* Endocrinology, 2000. **141**(7): p. 2691-7.

95. Fukuda, A., et al., *Effects of prolactin during preincubation of mouse spermatozoa on fertilizing capacity in vitro.* Journal of in Vitro Fertilization and Embryo Transfer, 1989. **6**(2): p. 92-97.

96. Postic, C., et al., *Dual roles for glucokinase in glucose homeostasis as determined by liver and pancreatic beta cell-specific gene knock-outs using Cre recombinase.* J Biol Chem, 1999. **274**(1): p. 305-15.

97. Chan, K., et al., *NRF2, a member of the NFE2 family of transcription factors, is not essential for murine erythropoiesis, growth, and development.* Proc Natl Acad Sci U S A, 1996. **93**(24): p. 13943-8.

98. Ormandy, C.J., et al., *Null mutation of the prolactin receptor gene produces multiple reproductive defects in the mouse.* Genes Dev, 1997. **11**(2): p. 167-78.

99. Yokota, S., et al., *Partial Bile Duct Ligation in the Mouse: A Controlled Model of Localized Obstructive Cholestasis.* J Vis Exp, 2018(133).

100. Rui, W., et al., *Nuclear Factor Erythroid 2-Related Factor 2 Deficiency Results in Amplification of the Liver Fat-Lowering Effect of Estrogen.* J Pharmacol Exp Ther, 2016. **358**(1): p. 14-21.

101. Haglund, F., et al., *Prolactin receptor in primary hyperparathyroidism--expression, functionality and clinical correlations.* PLoS One, 2012. **7**(5): p. e36448.

102. Mortlock, R.D., S.K. Georgia, and S.D. Finley, *Dynamic Regulation of JAK-STAT Signaling Through the Prolactin Receptor Predicted by Computational Modeling.* Cell Mol Bioeng, 2021. **14**(1): p. 15-30.

103. Bocchini, C.E., et al., *Contribution of chaperones to STAT pathway signaling.* Jakstat, 2014. **3**(3): p. e970459.

104. Britschgi, A., et al., *JAK2/STAT5 inhibition circumvents resistance to PI3K/mTOR blockade: a rationale for cotargeting these pathways in metastatic breast cancer.* Cancer Cell, 2012. **22**(6): p. 796-811.

105. Aleksunes, L.M., et al., *Nuclear factor-E2-related factor 2 expression in liver is critical for induction of NAD(P)H:quinone oxidoreductase 1 during cholestasis.* Cell Stress Chaperones, 2006. **11**(4): p. 356-63.

106. Buckman, M.T., G.T. Peake, and G. Robertson, *Hyperprolactinemia influences renal function in man.* Metabolism, 1976. **25**(5): p. 509-16.

107. Pala, N.A., et al., *Metabolic abnormalities in patients with prolactinoma: response to treatment with cabergoline.* Diabetol Metab Syndr, 2015. **7**: p. 99.

108. Shibli-Rahhal, A. and J. Schlechte, *The effects of hyperprolactinemia on bone and fat.* Pituitary, 2009. **12**(2): p. 96-104.

109. Diegelmann, J., et al., *A novel role for interleukin-27 (IL-27) as mediator of intestinal epithelial barrier protection mediated via differential signal transducer and activator of transcription (STAT) protein signaling and induction of antibacterial and anti-inflammatory proteins.* J Biol Chem, 2012. **287**(1): p. 286-298.

110. Damiri, B., et al., *Lentiviral-mediated RNAi knockdown yields a novel mouse model for studying Cyp2b function.* Toxicol Sci, 2012. **125**(2): p. 368-81.

111. Dovrtelova, G., et al., *Effect of Endocannabinoid Oleamide on Rat and Human Liver Cytochrome P450 Enzymes in In Vitro and In Vivo Models.* Drug Metab Dispos, 2018. **46**(6): p. 913-923.

112. Jahn, G.A., et al., *In vivo study of prolactin (PRL) intracellular signalling during lactogenesis in the rat: JAK/STAT pathway is activated by PRL in the mammary gland but not in the liver.* Biol Reprod, 1997. **57**(4): p. 894-900.

113. Reichold, A., et al., *Dmbt1 does not affect a Western style diet-induced liver damage in mice.* J Clin Biochem Nutr, 2013. **53**(3): p. 145-9.

114. Qian, H., et al., *An HNF1α-regulated feedback circuit modulates hepatic fibrogenesis via the crosstalk between hepatocytes and hepatic stellate cells.* Cell Res, 2015. **25**(8): p. 930-45.

115. Deng, H., et al., *Expression of deleted in malignant brain tumours 1 (DMBT1) relates to the proliferation and malignant transformation of hepatic progenitor cells in hepatitis B virus-related liver diseases.* Histopathology, 2012. **60**(2): p. 249-60.

116. Siegel, D., et al., *Redox modulation of NQO1.* PLoS One, 2018. **13**(1): p. e0190717.